



1 **A modeling study of the nonlinear response of fine**
2 **particles to air pollutant emissions in the Beijing-Tianjin-**
3 **Hebei region**

4
5 **Bin Zhao^{1,2,3}, Wenjing Wu^{1,2}, Shuxiao Wang^{1,2}, Jia Xing^{1,2}, Xing Chang^{1,2}, Kuo-**
6 **Nan Liou³, Jonathan H. Jiang⁴, Yu Gu³, Carey Jang⁵, Joshua S. Fu⁶, Yun Zhu⁷,**
7 **Jiandong Wang^{1,2}, Jiming Hao^{1,2}**

8 [1] School of Environment, and State Key Joint Laboratory of Environment Simulation and
9 Pollution Control, Tsinghua University, Beijing 100084, China

10 [2] State Environmental Protection Key Laboratory of Sources and Control of Air Pollution
11 Complex, Beijing 100084, China

12 [3] Joint Institute for Regional Earth System Science and Engineering and Department of
13 Atmospheric and Oceanic Sciences, University of California, Los Angeles, CA 90095, USA

14 [4] Jet propulsion Laboratory, California Institute of Technology, Pasadena, CA 91109, USA

15 [5] U.S. Environmental Protection Agency, Research Triangle Park, NC 27711, USA

16 [6] Department of Civil and Environmental Engineering, University of Tennessee, Knoxville,
17 TN 37996, United States

18 [7] School of Environmental Science and Engineering, South China University of
19 Technology, Guangzhou 510006, China

20

21

22 Correspondence to: Shuxiao Wang (shxwang@tsinghua.edu.cn)

23

24 **Abstract.**

25 The Beijing-Tianjin-Hebei (BTH) region has been suffering from the most severe fine particle
26 (PM_{2.5}) pollution in China, which causes serious health damage and economic loss.
27 Quantifying the source contributions to PM_{2.5} concentrations has been a challenging task
28 because of the complicated non-linear relationships between PM_{2.5} concentrations and
29 emissions of multiple pollutants from multiple spatial regions and economic sectors. In this
30 study, we use the Extended Response Surface Modeling (ERSM) technique to investigate the



1 nonlinear response of $PM_{2.5}$ and its major chemical components to emissions of multiple
2 pollutants from different regions and sectors over the BTH region, based on over 1000
3 simulations by a chemical transport model (CTM). The ERSM-predicted $PM_{2.5}$ concentrations
4 agree well with independent CTM simulations, with correlation coefficients larger than 0.99
5 and mean normalized errors less than 1%. Using the ERSM technique, we find that primary
6 inorganic $PM_{2.5}$ is the single pollutant which makes the largest contribution (24-36%) to $PM_{2.5}$
7 concentrations. The contribution of primary inorganic $PM_{2.5}$ emissions is especially high in
8 heavily polluted winter, and is dominated by the industry as well as residential and
9 commercial sectors, which should be prioritized in $PM_{2.5}$ control strategies. The total
10 contributions of all precursors (nitrogen oxides, NO_x ; sulfur dioxides, SO_2 ; ammonia, NH_3 ;
11 non-methane volatile organic compounds, NMVOC; intermediate-volatility organic
12 compounds, IVOC; primary organic aerosol, POA) to $PM_{2.5}$ concentrations range between 31%
13 and 48%. Among these precursors, $PM_{2.5}$ concentrations are primarily sensitive to the
14 emissions of NH_3 , NMVOC+IVOC, and POA. The sensitivities increase substantially for NH_3
15 and NO_x , and decrease slightly for POA and NMVOC+IVOC with the increase in the
16 emission reduction ratio, which illustrates the nonlinear relationships between precursor
17 emissions and $PM_{2.5}$ concentrations. The contributions of primary inorganic $PM_{2.5}$ emissions
18 to $PM_{2.5}$ concentrations are dominated by local emission sources, which account for over 75%
19 of the total primary inorganic $PM_{2.5}$ contributions. For precursors, however, emissions from
20 other regions could play similar roles as local emission sources in the summer and over the
21 northern part of BTH. The source contribution features for various types of heavy-pollution
22 episodes are distinctly different from each other, and from the monthly mean results,
23 illustrating the need of discrepant temporary control strategies for different pollution types.

24

25 **1 Introduction**

26 China is one of the regions with highest concentration of $PM_{2.5}$ (particulate matter with
27 aerodynamic diameter equal to or less than $2.5 \mu m$) in the world (van Donkelaar et al., 2015).
28 The problem is especially serious over the Beijing-Tianjin-Hebei (BTH) region, one of the
29 most populous and developed regions in China. Annual average $PM_{2.5}$ concentrations in this
30 region reached $85-110 \mu g/m^3$ during 2013-2015, which approximately triple the standard
31 threshold ($35 \mu g/m^3$) and far exceed those in other metropolitan regions (Wang et al., 2017). It
32 has been estimated that the severe $PM_{2.5}$ pollution leads to about 1.05-1.23 million premature



1 deaths per year in China (Lim et al., 2012; Burnett et al., 2014; Wang et al., 2016b), and the
2 monetized loss over the BTH region is as high as 134 billion Chinese Yuan, representing 2.2%
3 of regional gross domestic product (GDP) (Lv and Li, 2016). Additionally, PM_{2.5} substantially
4 affects global and regional climate by absorbing and scattering solar radiation and by altering
5 cloud properties (Stocker et al., 2013).

6 To tackle the heavy PM_{2.5} pollution problem, Chinese government issued the "Action Plan
7 on Prevention and Control of Air Pollution" in September 2013, which aimed at a 25%
8 reduction in PM_{2.5} concentrations over the BTH region by 2017 from the 2012 levels (The
9 State Council of the People's Republic of China, 2013). The attainment of ambient PM_{2.5}
10 standard would further require substantial reductions in air pollutant emissions (Wang et al.,
11 2017). To establish emission control strategies, many studies have apportioned the sources of
12 PM_{2.5} over the BTH region, either by mining monitoring data using the Positive Matrix
13 Factorization and Chemical Mass Balance methods (e.g., Zhang et al., 2007; Yu et al., 2013)
14 or by embedding chemical tracers in chemical transport models (CTMs) (e.g., Wang et al.,
15 2016c; Li et al., 2015b; Ying et al., 2014). While these studies can capture the current
16 contributions of various sources to PM_{2.5} concentrations, these contributions could differ
17 significantly from the PM_{2.5} reductions induced by reducing emissions from the corresponding
18 sources, due to highly nonlinear chemical mechanisms (Han et al., 2016; Wang et al., 2011).
19 Therefore, it is imperative to assess the nonlinear response of PM_{2.5} to pollutant emissions
20 from multiple sources, which could provide direct support for the development of effective
21 control policies.

22 CTMs are the only feasible tools for evaluating the response of PM_{2.5} concentrations to
23 emission changes (Hakami et al., 2003). The most widely used technique to evaluate these
24 responses is the "Brute force" method, which involves perturbing emissions from a certain
25 source and repeated solution of the model (Russell et al., 1995). A number of studies have
26 utilized the "Brute force" method to quantify the contributions of emissions from different
27 spatial regions (Streets et al., 2007; Wang et al., 2008; Li and Han, 2016; Wang et al., 2014a),
28 or different economic sectors (Wang et al., 2008; Han et al., 2016; Wang et al., 2014a; Liu et
29 al., 2016) to PM_{2.5} concentrations over the BTH region, either on a seasonal basis (Streets et
30 al., 2007; Wang et al., 2008; Han et al., 2016; Liu et al., 2016) or during a specific heavy-
31 pollution episode (Li and Han, 2016; Wang et al., 2014a). To improve the computational
32 efficiency, several mathematic techniques embedded in CTMs have been developed to



1 simultaneously calculate the sensitivities of the modeled concentrations to multiple emission
2 sources, including the Decoupled Direct Method (Yang et al., 1997) and Adjoint Analysis
3 (Sandu et al., 2005; Hakami et al., 2006). Zhang et al. (2016) used the Adjoint Analysis
4 method to examine sensitivities of $PM_{2.5}$ concentrations in the BTH region to pollutant
5 emissions during several pollution periods. However, these studies have inadequately
6 captured the nonlinearity in the responses of $PM_{2.5}$ concentrations to pollutant emissions,
7 which can be extremely strong due to complex chemical mechanisms (Wang et al., 2011).
8 Moreover, no studies have simultaneously evaluated the response of $PM_{2.5}$ concentrations in
9 BTH to emissions of multiple pollutants from different sectors and regions, which we need to
10 consider and balance to develop cost-effective control strategies.

11 In light of the drawbacks of the preceding methods, the Response Surface Modeling
12 (RSM) technique (denoted by “conventional RSM” technique hereafter to distinguish from
13 the ERSM technique) has been developed by using advanced statistical techniques to
14 characterize the nonlinear relationship between model outputs and inputs (U.S. Environmental
15 Protection Agency, 2006; Xing et al., 2011; Wang et al., 2011). This technique has been
16 applied to the United States (U.S. Environmental Protection Agency, 2006) and the Eastern
17 China (Wang et al., 2011) to evaluate the response of $PM_{2.5}$ and its chemical components to
18 pollutant emissions. Recently, we developed the Extended Response Surface Modeling
19 (ERSM) technique (Zhao et al., 2015b), which substantially extended the applicability of
20 conventional RSM to an increased number of variables and geographical regions with an
21 acceptable amount of computational burden.

22 Given the advantage of the ERSM technique, here we apply it to over 1000 simulations by
23 the Community Multi-scale Air Quality model with Two-Dimensional Volatility Basis Set
24 (CMAQ/2D-VBS) to systematically evaluate the nonlinear response of $PM_{2.5}$ and its major
25 chemical components to emission changes of multiple pollutants from different sectors and
26 regions over the BTH region. The major sources contributing to $PM_{2.5}$ and its major
27 components are identified and the nonlinearity in the response of $PM_{2.5}$ to emission changes is
28 characterized. Based on results of this study, suggestions for $PM_{2.5}$ control policies over the
29 BTH region are proposed.



1 **2 Methodology**

2 **2.1 CMAQ/2D-VBS configuration and evaluation**

3 The CMAQ/2D-VBS model was developed in our previous study (Zhao et al., 2016) by
4 incorporating the 2D-VBS model framework into CMAQv5.0.1. Compared with the default
5 CMAQ, the CMAQ/2D-VBS model explicitly simulates aging of secondary organic aerosol
6 (SOA) formed from non-methane volatile organic compounds (NMVOC), aging of primary
7 organic aerosol (POA), and photo-oxidation of intermediate-volatility organic compounds
8 (IVOC), thereby significantly improving the simulation results of organic aerosol (OA) and
9 SOA. The model parameters within the 2D-VBS framework have been optimized in our
10 previous studies (Zhao et al., 2015a; Zhao et al., 2016) based on a series of smog-chamber
11 experiments. Here we use the same model parameters as those of the “High-Yield VBS”
12 configuration reported in Zhao et al. (2016), which agrees best with surface OA and SOA
13 observations among three model configurations. An application in the Eastern China reveals
14 that CMAQ/2D-VBS reduces the underestimation in OA concentrations from 45% (default
15 CMAQv5.0.1) to 19%. More importantly, while the default CMAQv5.0.1 substantially
16 underestimates the fraction of SOA in OA by 5–10 times and can not track oxygen-to-carbon
17 ratio (O:C), the SOA fraction and O:C simulated by CMAQ/2D-VBS agree fairly well with
18 observations.

19 We apply the CMAQ/2D-VBS model over the BTH region. One-way, double nesting
20 simulation domains are used, as shown in Fig. 1. Domain 1 covers East Asia with a grid
21 resolution of 36 km×36 km; domain 2 covers the BTH and its surrounding regions with a grid
22 resolution of 12 km×12 km. We use the SAPRC99 gas-phase chemistry module and the
23 AERO6 aerosol module, in which the treatment of OA is replaced with the 2D-VBS
24 framework. The aerosol thermodynamics is based on ISORROPIA-II. The initial and
25 boundary conditions for Domain 1 are kept constant as the model default profile, and those
26 for Domain 2 are extracted from the output of Domain 1. A 5-day spin-up period is used to
27 reduce the influence of initial conditions on modeling results.

28 The Weather Research and Forecasting Model (WRF, version 3.7) is used to generate the
29 meteorological fields. The National Center for Environmental Prediction (NCEP)’s Final
30 Analysis reanalysis data at 1.0° × 1.0° and 6-h resolution are used to generate the first guess
31 field. The NCEP’s Automated Data Processing (ADP) data are used in the objective analysis
32 scheme. The major physics options for WRF include the Kain-Fritsch cumulus scheme, the



1 Pleim-Xiu land-surface module, the Asymmetric Convective Model with non-local upward
2 mixing and local downward mixing (ACM2) for planetary boundary layer (PBL)
3 parameterization, the Morrison double-moment scheme for cloud microphysics, and the Rapid
4 Radiative Transfer Model for GCMs (RRTMG) radiation scheme. Terrain and land use data
5 are obtained from the Moderate resolution Imaging Spectroradiometer (MODIS). The
6 simulation periods are January, March, July, and October in 2014, representing winter, spring,
7 summer, and fall. We select these four months because the occurrence frequencies of various
8 meteorological types in these months are statistically most similar to the average conditions in
9 winter, spring, summer, and fall during 2004-2013 (Wu, 2016).

10 A high-resolution anthropogenic emission inventory in 2014 has been developed using an
11 “emission factor method” (Fu et al., 2013; Zhao et al., 2013b) for the BTH region by
12 Tsinghua University. The emissions from area and mobile sources are first calculated for each
13 prefecture-level city based on statistical data, and subsequently distributed into the model
14 grids according to spatial distribution of population, GDP, and road networks. A unit-based
15 method (Zhao et al., 2008) is applied to estimate and locate the emissions from large point
16 sources (LPS) including power plants, iron and steel plants, and cement plants. The
17 anthropogenic emission inventory in other provinces of China was originally developed for
18 2010 and 2012 in our previous studies (Zhao et al., 2013b; Zhao et al., 2013a; Wang et al.,
19 2014b; Cai et al., 2016), which has been updated to 2014 in this study following the same
20 methodology. Table S1 summarizes emissions of major air pollutants in each prefecture-level
21 city over the BTH region in 2014; Table S2 gives the provincial emissions in the whole China
22 in 2014. The emissions for other countries are obtained from the MIX emission inventory (Li
23 et al., 2015a) for 2010, which is the latest year available. The biogenic emissions were
24 calculated by the Model of Emissions of Gases and Aerosols from Nature (MEGAN;
25 Guenther et al., 2006).

26 We compared the simulation results of WRFv3.7 and CMAQ/2D-VBS with
27 meteorological observations obtained from the National Climatic Data Center (NCDC), PM_{2.5}
28 observations at 138 state-controlled observational sites, and observations of major PM_{2.5}
29 chemical components at 7 sites within the modeling domain. We show that the meteorological
30 and chemical simulations generally agree well with observations, with performance statistics
31 mostly within the benchmark values proposed by previous studies. Details of the model



1 evaluation methods and results are given in the Supplementary Information (Section 1, Table
2 S3-S5, Fig. S1-S5).

3 **2.2 Development of ERSM prediction system**

4 The detailed methodologies of the conventional RSM and ERSM techniques have been
5 described in our previous papers (Zhao et al., 2015b; Xing et al., 2011). Here we only
6 summarize some key components. The conventional RSM technique characterizes the
7 relationships between a response variable (e.g., $PM_{2.5}$ concentration) and a set of control
8 variables (i.e., emissions of particular pollutants from particular sources) based on a number
9 of randomly generated emission control scenarios (Xing et al., 2011; Wang et al., 2011). The
10 $PM_{2.5}$ concentration for each emission scenario is calculated with a CTM (CMAQ/2D-VBS in
11 this study), and the conventional RSM is subsequently established using the Maximum
12 Likelihood Estimation - Empirical Best Linear Unbiased Predictors (MLE-EBLUPs)
13 developed by Santner et al. (2003). Due to the limitation of the conventional RSM technique
14 with respect to variable number, we have developed the ERSM technique (Zhao et al., 2015b)
15 to extend the applicability to an increased number of variables and geographical regions. The
16 ERSM technique first quantifies the relationship between $PM_{2.5}$ concentrations and precursor
17 emissions for each single region using the conventional RSM technique as described above,
18 and then assesses the effects of inter-regional transport of $PM_{2.5}$ and its precursors on $PM_{2.5}$
19 concentration in the target region. In order to quantify the interaction among regions, we
20 introduce a key assumption that the emissions of precursors in the source region affect $PM_{2.5}$
21 concentrations in the target region through two major processes: (1) the inter-regional
22 transport of precursors enhancing the chemical formation of secondary $PM_{2.5}$ in the target
23 region; (2) the formation of secondary $PM_{2.5}$ in the source region followed by transport to the
24 target region. We quantify the individual contributions of these two processes as well as the
25 contribution of local emissions in the target region, which are subsequently integrated to
26 derive the total $PM_{2.5}$ concentrations in the target region.

27 For application of the RSM/ERSM techniques to the BTH region, we define 5 target
28 regions in the inner modeling domain (Domain 2), i.e., Beijing, Tianjin, Northern Hebei (N
29 Hebei), Eastern Hebei (E Hebei), and Southern Hebei (S Hebei), as shown in Fig. 1. The
30 decomposition of the Hebei province is based on a preliminary analysis of the pollutant
31 transport patterns over the BTH region (Section 2 in the Supplementary Information). The
32 simulation using back trajectory method indicates that four major types of heavy-pollution



1 episodes in Beijing are primarily contributed by air mass from the south, the local area, the
2 northwest, and the southeast. We develop two RSM/ERSM prediction systems (Table 1). The
3 response variables for both of them are concentrations of $\text{PM}_{2.5}$, SO_4^{2-} , NO_3^- , and OA over the
4 urban areas of prefecture-level cities in the five target regions. The first prediction system use
5 the conventional RSM technique and 101 emission control scenarios generated by the Latin
6 Hypercube Sample (LHS) method (Iman et al., 1980) to map atmospheric concentrations
7 versus total emissions of NO_x , SO_2 , NH_3 , NMVOC+IVOC, and POA in all five target regions.
8 This prediction system is intended for the validation (Section 3.1) of the second system,
9 which is established using the ERSM technique. For the second system, the emissions of
10 $\text{PM}_{2.5}$ precursors and primary inorganic $\text{PM}_{2.5}$ in each of the 5 regions are categorized into 7
11 and 4 control variables, respectively, resulting in 55 control variables in total (see Table 1).
12 We generate 1121 scenarios (see Table 1) to build the response surface, following the method
13 detailed in Zhao et al. (2015b). Specifically, the scenarios include (1) 1 CMAQ/2D-VBS base
14 case; (2) 200 scenarios generated by applying LHS method for the control variables of
15 precursors in Beijing, 200×4 scenarios generated in the same way for Tianjin, Northern Hebei,
16 Eastern Hebei, and Southern Hebei; (3) 100 scenarios generated by applying LHS method for
17 the total emissions of NO_x , SO_2 , NH_3 , NMVOC+IVOC, and POA in all 5 regions; and (4) 20
18 scenarios where one of the control variables of primary inorganic $\text{PM}_{2.5}$ emissions is set to
19 0.25 for each scenario. Here the scenario numbers (200 in group 2 and 100 in group 3) are
20 determined based on numerical experiments conducted in our previous studies (Xing et al.,
21 2011; Wang et al., 2011), which showed that the response surface for 7 and 5 variables could
22 be built with good prediction performance (mean normalized error < 1%; correlation
23 coefficient > 0.99) using 200 and 100 scenarios, respectively. Finally, we generate 54
24 independent scenarios for out-of-sample validation, which will be detailed in Section. 3.1.

25 For application of the ERSM prediction system to quantitatively characterize the
26 sensitivity of $\text{PM}_{2.5}$ concentrations to emission changes, we define “ $\text{PM}_{2.5}$ sensitivity” as the
27 change ratio of $\text{PM}_{2.5}$ concentration divided by the reduction ratio of a emission source,
28 following previous studies (Zhao et al., 2015b; Wang et al., 2011).

$$29 \quad S_a^X = [(C^* - C_a) / C^*] / (1 - a) \quad (4)$$

30 where S_a^X is the $\text{PM}_{2.5}$ sensitivity to emission source X at its emission ratio a ; C^* and C_a are
31 $\text{PM}_{2.5}$ concentrations in the base case (when the emission ratio of X is 1) and in the control



1 scenario where the emission ratio of X is a , respectively. Similar indices can be defined for
2 chemical components of $PM_{2.5}$, such as NO_3^- , SO_4^{2-} , and OA.

4 3 Results and discussion

5 3.1 Validation of ERSM performance

6 The performance of the conventional RSM technique has been well evaluated in our previous
7 papers (Xing et al., 2011; Wang et al., 2011), so we only describe the validation of the ERSM
8 technique. Following Zhao et al. (2015b), we assess the performance of the ERSM prediction
9 system using the “out-of-sample” and 2D-isopleths validation methods, which focus on the
10 accuracy and stability of the prediction system, respectively.

11 For out-of-sample validation, we use the ERSM prediction system to calculate the $PM_{2.5}$
12 concentrations for 54 “out-of-sample” control scenarios, i.e., scenarios independent from
13 those used to build the prediction system, and compare with the corresponding CMAQ/2D-
14 VBS simulation results. These 54 out-of-sample scenarios (summarized in Table S6) include
15 40 cases (case 1-40) where the control variables of precursors change but those of primary
16 inorganic $PM_{2.5}$ stay the same as the base case, 4 cases (case 41-44) the other way around, and
17 10 cases (case 45-54) where control variables of precursors and primary inorganic $PM_{2.5}$
18 change simultaneously. Most cases are generated randomly with the LHS method (case 4-6,
19 10-12, 16-18, 22-24, 28-54), and some cases are designed where all control variables are
20 subject to large emission changes (case 1-3, 7-9, 13-15, 19-21, 25-27).

21 Figure 2 compares the ERSM-predicted and CMAQ/2D-VBS-simulated $PM_{2.5}$
22 concentrations for the out-of-sample scenarios using scattering plots. Table 2 summarizes the
23 statistics of the model performance. The definitions of normalized error (NE), mean
24 normalized error (MNE), and normalized mean error (NME) are given as follows:

$$25 \quad NE = |P_i - S_i| / S_i \quad (1)$$

$$26 \quad MNE = \frac{1}{N_s} \sum_{i=1}^{N_s} [|P_i - S_i| / S_i] \quad (2)$$

$$27 \quad NME = \sum_{i=1}^{N_s} |P_i - S_i| / \sum_{i=1}^{N_s} S_i \quad (3)$$

28 where P_i and S_i are the ERSM-predicted and CMAQ/2D-VBS-simulated value of the i^{th} out-
29 of-sample scenario; N_s is the number of out-of-sample scenarios. Figure 2 shows that the
30 ERSM predictions and CMAQ/2D-VBS simulations agree well with each other. The
31 correlation coefficients are larger than 0.99, and the MNEs and NMEs are less than 1% for all



1 four months. The maximum NEs could be as large as 11% for particular month and region,
2 but the 95% percentiles of NEs are all within 4.4%. NEs exceeding 4.4% happen only for the
3 scenarios where most control variables are reduced substantially, indicating relatively large
4 errors at low emission rates, which is consistent with our previous study (Zhao et al., 2015b).
5 Note that all sensitivity scenarios used in Sections 3.2-3.4 have $\leq 80\%$ emission reductions,
6 which helps to avoid relatively large errors. We also examine the errors in predicted $PM_{2.5}$
7 response, which is defined as the difference between $PM_{2.5}$ concentration in an emission
8 control scenario and that in the base case. Table 2 shows that the NMEs of $PM_{2.5}$ response are
9 within 5.6% for all months. In summary, the out-of-sample validation indicates an overall
10 good agreement between ERSM predictions and CMAQ/2D-VBS simulations.

11 We further examine whether the ERSM technique can capture the trends in $PM_{2.5}$
12 concentrations in response to continuous changes in precursor emissions, i.e., the stability of
13 the ERSM technique. To this end, we compare the 2D-isopleths of $PM_{2.5}$ concentrations as a
14 function of simultaneous changes in two precursors' emissions in all five regions derived
15 from the ERSM and conventional RSM techniques; the stability of the latter has been fully
16 demonstrated (Xing et al., 2011; Wang et al., 2011). Figure 3 illustrates the $PM_{2.5}$ isopleths in
17 Beijing as a function of three combinations of precursors, i.e., NO_x vs NH_3 , SO_2 vs NH_3 , and
18 $VOC+IVOC$ vs POA ; the isopleths for other regions are very similar and thus not shown. The
19 X- and Y-axis of the figures represent the "emission ratio", defined as the ratios of the
20 changed emissions to the emissions in the base case. For example, an emission ratio of 0.7
21 means the emission of a particular control variable accounts for 70% that of the base case.
22 The colour isopleths represent $PM_{2.5}$ concentrations. The comparison shows that the shapes of
23 isopleths derived from both prediction systems generally agree with each other. The
24 agreement is very good for the case of $VOC+IVOC$ vs POA , and for the cases of NO_x vs NH_3
25 and SO_2 vs NH_3 when the emission ratios for NO_x and NH_3 are larger than 0.2. Relatively
26 large errors occur at low NO_x/NH_3 emission ratios (< 0.2) due primarily to a very strong
27 nonlinearity in these emission ranges. For application in control policy analysis, $> 80\%$
28 emission reductions are extremely rare as limited by the technologically feasible reduction
29 potentials (Wang et al., 2014b). The general consistency between RSM and ERSM-predicted
30 isopleths demonstrates the stability of the ERSM prediction system. In other words, although
31 the ERSM predictions are definitely subject to numerical errors, these errors could not
32 challenge the major conclusions on the effectiveness of emission reductions.



1 **3.2 Response of PM_{2.5} concentrations to emissions of air pollutants**

2 Having demonstrated the reliability of the ERSM prediction system, we employ it to
3 investigate the responses of PM_{2.5} concentrations to emissions of various pollutants from
4 different sectors and regions. We use “PM_{2.5} sensitivity” defined in Section 2.2 to
5 quantitatively characterize the sensitivity of PM_{2.5} concentrations to emission changes. Figure
6 4 illustrates the sensitivity of 4-month (January, March, July, and October) mean PM_{2.5}
7 concentrations to stepped control of individual air pollutants and individual pollutant-sector
8 combinations in the BTH region, which are derived from the ERSM technique. Among all
9 pollutants, the 4-month mean PM_{2.5} concentrations are most sensitive to the emissions of
10 primary inorganic PM_{2.5} in all five regions, and the PM_{2.5} sensitivities vary from 24% to 36%
11 according to region. When primarily inorganic PM_{2.5} emissions from various sectors are
12 differentiated, the industry sector is found to make the largest contribution to PM_{2.5}
13 concentrations, followed by the residential and commercial sectors; the contribution of power
14 plants is negligibly small because of smaller emissions and higher stacks. The PM_{2.5}
15 sensitivities to primarily inorganic PM_{2.5} emissions remain constant at various reduction ratios.

16 While primary inorganic PM_{2.5} represents the single pollutant which makes the largest
17 contribution to PM_{2.5} concentrations, the total contributions of all precursors (NO_x, SO₂, NH₃,
18 NMVOC, IVOC, and POA), which range between 31% and 48%, exceed that of primary
19 inorganic PM_{2.5} (24-36%). Among the precursors, PM_{2.5} concentrations are primarily sensitive
20 to the emissions of NH₃, NMVOC+IVOC, and POA, and their relative importance differ
21 according to reduction ratio. The PM_{2.5} sensitivity to NH₃ increases substantially with the
22 increase of reduction ratio, primarily attributable to the transition from NH₃-rich to NH₃-poor
23 regimes when more controls are enforced. The PM_{2.5} sensitivities to POA and NMVOC+IVOC,
24 however, decrease slightly with the increase of reduction ratio. This is because that, based on
25 the gas-particle absorptive partitioning theory, organics have a higher tendency to partition
26 into the particle phase at larger OA concentrations. As a result of the nonlinearity, the PM_{2.5}
27 sensitivities to POA and NMVOC+IVOC emissions are larger than those to NH₃ emissions at
28 small reduction ratios (e.g., 20%), while it is the other way around at large reduction ratios
29 (e.g., 80%). The PM_{2.5} sensitivity to SO₂ emissions is considerably smaller compared with the
30 three precursors above, and does not change significantly as a function of reduction ratio. The
31 response of PM_{2.5} concentrations to NO_x emissions could change from negative to positive
32 with the increase of reduction ratio, which has been reported in several previous studies



1 (Dong et al., 2014; Zhao et al., 2013c; Cai et al., 2016). Small NO_x emission reductions could
2 lead to increase in O_3 and HO_x concentrations in several seasons owing to a NMVOC-limited
3 photochemical regime, which on one hand enhances SO_4^{2-} and SOA formation, and on the
4 other hand, could also increase NO_3^- concentrations by accelerating the nocturnal formation of
5 N_2O_5 and HNO_3 through the $\text{NO}_2 + \text{O}_3$ reaction at low temperatures. A substantial reduction
6 in NO_x emissions, however, transforms the NMVOC-limited regime to a NO_x -limited regime,
7 resulting in a successive decline in concentrations of O_3 , HO_x , and most $\text{PM}_{2.5}$ chemical
8 components. In addition, the responses of $\text{PM}_{2.5}$ concentrations to NO_x emission changes are
9 discrepant in different regions. For example, NO_x emission reductions can mostly lead to
10 $\text{PM}_{2.5}$ decline in Northern Hebei, because this region, which is the northernmost region within
11 BTH, is substantially affected by emissions in other regions. Considering that the
12 photochemistry typically changes from a NMVOC-limited regime in urban areas at surface to
13 a NO_x -limited regime in rural areas or at upper levels (Xing et al., 2011), the NO_x emission
14 reductions in upwind regions are more likely to result in a net $\text{PM}_{2.5}$ decline compared with
15 local emission reductions. Note that NO_x emissions were recently found to oxidize SO_2 in
16 aerosol water, leading to additional $\text{PM}_{2.5}$ formation (Cheng et al., 2016; Wang et al., 2016a).
17 Incorporation of this process in the model may affect the simulated response of $\text{PM}_{2.5}$ to NO_x
18 emissions. Regarding emission sectors, the contributions of SO_2 and NO_x emissions are
19 dominated by “other sources” (sources other than LPS) because they emit larger amount of
20 pollutants at lower height compared with LPS. When all pollutants are controlled together, the
21 $\text{PM}_{2.5}$ sensitivity generally increases with reduction ratio, indicating that additional air quality
22 benefit could be achieved, larger than the expectation from linear extrapolation, if more
23 control measures are implemented.

24 Figure 5 illustrates the $\text{PM}_{2.5}$ sensitivities to individual pollutant-sector combinations in
25 each month. The source contribution features are significantly discrepant in different months.
26 The contributions of primary inorganic $\text{PM}_{2.5}$ emissions to $\text{PM}_{2.5}$ concentrations are notably
27 higher in January than in other months, which is probably attributed to weaker dilution and
28 slower chemical reactions in January. Regarding different emission sectors of primary
29 inorganic $\text{PM}_{2.5}$, the industrial sector plays a dominant role in all months except January,
30 when the residential and commercial sectors make a similar or even larger contribution as
31 compared to the industrial sector. This result highlights the importance of low-level
32 residential and commercial sources for $\text{PM}_{2.5}$ pollution controls in the winter. The



1 contributions of precursors are dominated by POA and NMVOC+IVOC in January, while in
2 July, NO_x , SO_2 , and NH_3 , which are known to be precursors of secondary inorganic aerosols,
3 make larger contributions than POA and NMVOC+IVOC. The responses of $\text{PM}_{2.5}$
4 concentrations to NO_x emissions can be opposite in different seasons. Specifically, in July,
5 NO_x emission reductions always induce decrease in $\text{PM}_{2.5}$ concentrations due to a NO_x -
6 limited photochemical regime. In January, however, even a 80% reduction in NO_x emissions
7 (roughly the maximum technically feasible reduction ratio) could result in a net $\text{PM}_{2.5}$ increase,
8 as a result of a strong NMVOC-limited regime. To achieve a net $\text{PM}_{2.5}$ reduction in January, it
9 would be necessary to simultaneously reduce NO_x emissions outside the BTH region.

10 We further evaluate the contributions of primary inorganic $\text{PM}_{2.5}$ and precursor emissions
11 from various regions to $\text{PM}_{2.5}$ concentrations (Fig. 6, Fig. S6). Here the contributions are
12 quantified by comparing the base case with sensitivity scenarios in which emissions from a
13 specific source are reduced by 80%, which reaches the maximum technologically feasible
14 reduction ratios of major pollutants in most areas (Wang et al., 2014b). Obviously, the
15 contributions of total primary inorganic $\text{PM}_{2.5}$ emissions in the BTH region are dominated by
16 local sources, which account for over 75% of the total primary inorganic $\text{PM}_{2.5}$ contributions.
17 When precursor emissions are decomposed into different regions, local sources usually also
18 represent the largest contributors, but precursor emissions from other regions (denoted by
19 “regional precursor emissions” hereafter) could also make significant contributions,
20 depending on seasons and regions. The importance of regional precursor emissions relative to
21 local ones is remarkably higher in July and over the northern part of BTH (e.g., Northern
22 Hebei, Beijing) than in January and over the southern part of BTH (e.g., Southern Hebei).
23 Over the BTH region, heavy pollution is frequently associated with southerly wind while
24 strong northerly wind often blows away $\text{PM}_{2.5}$ pollution (Jia et al., 2008; Zheng et al., 2015),
25 which explains the higher importance of regional precursor emissions in the northern part of
26 BTH. The higher regional contributions in the summer can be explained by the southerly
27 monsoon and stronger vertical mixing favoring inter-regional transport of air pollutants. We
28 also examine the contributions of emissions outside the BTH region to $\text{PM}_{2.5}$ concentrations in
29 the five target regions. The results reveal that these emissions contribute 24-33% of the 4-
30 month mean $\text{PM}_{2.5}$ concentrations, among which more than 80% could be attributed to
31 precursor emissions. Among the four months, the contribution of emissions outside BTH is
32 considerably smaller in January (12-21%) as compared to other months (29-38%).



1 **3.3 Response of PM_{2.5} chemical components to emissions of air pollutants**

2 Ambient PM_{2.5} is comprised of complicated chemical components with distinctly different
3 formation pathways. To gain deeper insight into the formation mechanisms and source
4 attribution of PM_{2.5}, we examine the sensitivities of major PM_{2.5} components, including NO₃⁻,
5 SO₄²⁻, and OA, to stepped control of individual air pollutants, as shown in Fig. 7 (January and
6 July) and Fig. S7 (March and October). NO₃⁻ concentrations are most sensitive to NH₃
7 emissions in all months except July, when the sensitivities of NO₃⁻ concentrations to NH₃ and
8 NO_x emissions are similar. The NO₃⁻ sensitivities to NO_x emissions differ significantly
9 according to season. In most months, NO₃⁻ concentrations are positively correlated with NO_x
10 emissions. In January, however, the sensitivities of NO₃⁻ concentrations to NO_x emissions are
11 mostly negative and could be positive at large reduction ratios, which can be explained by a
12 very strong NMVOC-limited photochemical regime, and abundant ice water for
13 heterogeneous formation of HNO₃ from N₂O₅ at cold temperatures. The sensitivities of NO₃⁻ to
14 both NH₃ and NO_x emissions show pronounced increasing trends with the increase of
15 reduction ratio, in agreement with the strong nonlinearity in these two pollutants described in
16 Section 3.2. NMVOC emissions make moderate positive contributions to NO₃⁻, with the
17 largest and smallest contributions occurring in January and July in conjunction with NMVOC-
18 limited and NO_x-limited photochemical regimes, respectively. Finally, SO₂ emissions have
19 very small influences on NO₃⁻ concentrations.

20 For SO₄²⁻, SO₂ emissions represent the dominant contributor in all months. The sensitivity
21 of SO₄²⁻ concentrations to SO₂ emissions does not change significantly with respect to
22 reduction ratio, consistent with the results shown in Section 3.2. The contributions of NH₃
23 emissions to SO₄²⁻ concentrations are quite small except in October, when NH₃ accounts for
24 approximately one fourth the contribution of SO₂. NO_x emissions affect SO₄²⁻ concentrations
25 by altering O₃ and HO_x concentrations (photochemical pathway) as well as by competing
26 with SO₂ for NH₃ (thermodynamic pathway). The overall net effects of these two pathways
27 are mostly negative, with positive effects occurring only in July at large reduction ratios.
28 NMVOC emissions can impose small impact on SO₄²⁻ concentrations primarily through
29 changing O₃ and HO_x concentrations.

30 The emissions of POA and NMVOC+IVOC are obviously two major contributors to OA
31 concentrations. The relative importance of the two is strongly dependent on season. In July,
32 POA and NMVOC+IVOC make similar contributions to OA concentrations, while POA



1 usually contributes more in other months. In January, the contribution of POA could account
2 for about four times those of NMVOC+IVOC. Similar to SO_4^{2-} , the impact of NO_x emissions
3 on OA concentrations also works through two pathways. Besides the abovementioned
4 photochemical pathway, NO_x emission reductions could lead to OA increases due to the fact
5 that SOA yield, defined as the ratio of SOA formation to the consumption of a precursor, is
6 generally higher at a low- NO_x condition than at a high- NO_x condition. As an integrated effect,
7 the responses of OA concentrations to NO_x emissions are negative in most situations.

8 **3.4 $\text{PM}_{2.5}$ responses to emission reductions during heavy-pollution episodes**

9 Having shown the responses of monthly-mean $\text{PM}_{2.5}$ concentrations to pollutant emissions,
10 we are also interested in heavy-pollution episodes, in which the source contributions could be
11 quite different from the monthly-mean results, largely due to variations in meteorological
12 conditions. To provide more insight into the control strategies for heavy pollution, we use the
13 ERSM technique to investigate the source contribution features during three typical heavy-
14 pollution episodes. We first select 47 heavy-pollution episodes over the BTH region during
15 2013-2015 (Table S7). Subsequently, we employ the Hybrid Single Particle Lagrangian
16 Integrated Trajectory (HYSPLIT) model (Stein et al., 2015) and Concentration Weighted
17 Trajectory (CWT) method (Cheng et al., 2013) to identify the potential source regions for
18 $\text{PM}_{2.5}$ during each episode, and categorize these episodes according to their source regions.
19 We then select a representative episode from each of three most important pollution types in
20 which the air mass primarily originates from local areas (“Local” type), from the south
21 (“South” type), and from the southeast (“Southeast” type). We give preference to episodes
22 within the four-month simulation period of this study to facilitate a comparison with the
23 monthly-mean source contribution features. For this reason, we select (1) January 5-7, 2014,
24 (2) October 7-11, 2014, and (3) October 29-31, 2014 as representatives of the “Local”,
25 “South”, and “Southeast” types. The selection of heavy-pollution episodes is detailed in
26 Section 2 of the Supplementary Information.

27 Figure 8 shows the contribution of precursor and primary inorganic $\text{PM}_{2.5}$ emissions from
28 individual regions to $\text{PM}_{2.5}$ concentrations during the three heavy-pollution episodes, and Fig.
29 9 illustrates the sensitivity of $\text{PM}_{2.5}$ concentrations to stepped control of individual pollutant-
30 sector combinations. During January 5-7, 2014 (“Local” type), the contributions of local
31 emission sources to $\text{PM}_{2.5}$ concentrations far exceed those from other regions within BTH as
32 well as from outside of BTH (Fig. 8). In contrast to the monthly mean results (Section 3.2),



1 the contributions of primary inorganic $PM_{2.5}$ emissions are comparable to, and even larger
2 than those of precursor emissions in the BTH region. The total contributions of primary $PM_{2.5}$
3 (including POA) account for as high as 70-80% of the contributions of all pollutants within
4 the BTH region, which highlights the crucial importance of primary $PM_{2.5}$ controls during this
5 episode. Moreover, the controls of NMVOC, NH_3 , and SO_2 emissions could contribute
6 moderately to reducing $PM_{2.5}$ concentrations. However, NO_X emission reduction induces an
7 increase in $PM_{2.5}$ concentrations, even at an 80% reduction ratio. Therefore, effective
8 temporary control measures for this episode should focus on the controls of local emissions,
9 with emphasis laid on primary $PM_{2.5}$.

10 During October 7-11, 2014 (“South” type), the contributions of emissions outside BTH to
11 $PM_{2.5}$ concentrations are as large as 33% in Beijing, and 40-50% in other regions. Within the
12 BTH region, the emissions from Southern Hebei can have similar effects to local emissions
13 on $PM_{2.5}$ concentrations in Beijing, indicating a strong long-range transport from the south. In
14 addition, the total contributions of precursor emissions about double those of primary
15 inorganic $PM_{2.5}$ emissions. Among all precursors, $PM_{2.5}$ concentrations are mainly sensitive to
16 emissions of NH_3 , NMVOC+IVOC, and POA. The sensitivity of $PM_{2.5}$ concentrations to NO_X
17 emissions increases dramatically with reduction ratio. Although small NO_X reductions may
18 slightly elevate $PM_{2.5}$ concentrations, large NO_X emission reduction (> 50%) can result in
19 significant $PM_{2.5}$ reduction. To effectively mitigate $PM_{2.5}$ pollution during this episode, we
20 should implement control measures for precursor emissions in both the BTH region
21 (especially the southern part) and regions south of BTH. The NO_X emissions, if controlled,
22 should be reduced by at least 50% to avoid adverse side effect.

23 For October 29-31, 2014 (“Southeast” type), $PM_{2.5}$ concentrations are also significantly
24 affected by emissions outside the BTH region. Within the BTH region, the $PM_{2.5}$
25 concentrations in Beijing and Northern Hebei are about equally affected by local emissions
26 and emissions from Eastern Hebei and Southern Hebei, while local emissions play dominant
27 roles in other regions. The emissions of both precursor and primary inorganic $PM_{2.5}$ within the
28 BTH region make important contributions to $PM_{2.5}$ concentrations, and the relative
29 significance of the two is dependent on region. All precursors except NO_X can contribute
30 considerably to $PM_{2.5}$ reductions, and the sensitivity of $PM_{2.5}$ to NH_3 increase rapidly with
31 emission ratio. NO_X emissions are negatively correlated with $PM_{2.5}$ concentrations in most
32 cases. Regarding the temporary control strategy for this episode, it is preferable to implement



1 joint controls of primary $\text{PM}_{2.5}$ and precursors both within and outside the BTH region, with
2 stringent measures over the Eastern and Southern Hebei.

3 From the analysis above, we conclude that the source contributions are tremendously
4 different in these three episodes, which have been demonstrated to represent some key
5 features of the corresponding pollution types (“Local”, “South”, and “Southeast” types).
6 Therefore, episode-specific control strategies need to be formulated based on the source
7 contribution features of individual pollution types. A caveat is that whether all conclusions
8 drawn from the three episodes can be generalized to the corresponding pollution types is still
9 uncertain. To gain a more comprehensive understanding of the source attribution and control
10 strategies of various heavy-pollution episodes, a model simulation of more episodes and a
11 more detailed classification appear warranted in future investigations.

12 **4 Conclusion and implications**

13 In the present study, we investigated the nonlinear response of $\text{PM}_{2.5}$ and its major chemical
14 components to emission changes of multiple pollutants from different sectors and regions
15 over the BTH region, using the ERSM technique coupled with the CMAQ/2D-VBS model.

16 Among individual pollutants, primary inorganic $\text{PM}_{2.5}$ makes the largest contribution (24-
17 36%) to the 4-month mean $\text{PM}_{2.5}$ concentrations. The contribution from primary inorganic
18 $\text{PM}_{2.5}$ is especially high in heavily polluted winter, and is dominated by the industry as well as
19 residential and commercial sectors. The total contributions of all precursors to $\text{PM}_{2.5}$
20 concentrations range between 31% and 48%. Among the precursors, $\text{PM}_{2.5}$ concentrations are
21 primarily sensitive to the emissions of NH_3 , NMVOC+IVOC, and POA. With the increase of
22 reduction ratio, the sensitivities of $\text{PM}_{2.5}$ concentrations to pollutant emissions remain roughly
23 constant for primary inorganic $\text{PM}_{2.5}$ and SO_2 , increase substantially for NH_3 and NO_x , and
24 decrease slightly for POA and NMVOC+IVOC. The contributions of primary inorganic $\text{PM}_{2.5}$
25 emissions to $\text{PM}_{2.5}$ concentrations are dominated by local emission sources, which account for
26 over 75% of the total primary inorganic $\text{PM}_{2.5}$ contributions. For precursors, however,
27 emissions from other regions could play similar roles to local emission sources in the summer
28 and over the northern part of BTH. Different $\text{PM}_{2.5}$ chemical components are associated with
29 distinct source contribution features. The NO_3^- and SO_4^{2-} concentrations are most sensitive to
30 emissions of NH_3 and SO_2 , respectively. The emissions of the POA and NMVOC+IVOC are
31 two major contributors to OA concentrations, with their relative importance depending on
32 season.



1 The source contribution features are significantly different for three typical heavy-
2 pollution episodes, which belong to three distinct pollution types. The $PM_{2.5}$ concentrations in
3 the first episode (“Local” type) are dominated by local sources and primary $PM_{2.5}$ emissions,
4 while the second episode (“South” type) is primarily affected by precursor emissions from
5 local and southern regions. The third episode (“Southeast” type) is significantly influenced by
6 emissions of both primary inorganic $PM_{2.5}$ and precursors from multiple regions. Future
7 investigations are needed to acquire generalized patterns for the source contributions of
8 various heavy-pollution types.

9 The results of the present study have important implications for $PM_{2.5}$ control policies
10 over the BTH region. First, the controls of primary $PM_{2.5}$ emissions should be a priority in
11 $PM_{2.5}$ control strategies. Primary $PM_{2.5}$, including primary inorganic $PM_{2.5}$ and POA,
12 contribute over half of the 4-month mean $PM_{2.5}$ concentrations, which is even higher in the
13 winter when heavy pollution frequently occurs. The industry sector and the residential and
14 commercial sectors represent 85% of the total primary $PM_{2.5}$ emissions, and therefore should
15 be the focus of primary $PM_{2.5}$ controls. In particular, we should pay special attention to the
16 residential and commercial sectors, which account for half of the total contribution of primary
17 $PM_{2.5}$ emissions to $PM_{2.5}$ concentrations in the winter but have been frequently neglected in
18 China’s previous control policies. Second, the control policies for NMVOC and IVOC
19 emissions should be strengthened. The sensitivity of $PM_{2.5}$ concentrations to NMVOC+IVOC
20 is one of the largest among all precursors. In particular, the controls of NMVOC and IVOC
21 emissions are very effective for $PM_{2.5}$ reduction even at the initial control stage, as indicated
22 by the large sensitivity at small reduction ratios. Moreover, NMVOC reduction is also crucial
23 for the mitigation of O_3 pollution considering a NMVOC-limited regime over the urban and
24 its surrounding areas (Xing et al., 2011). Third, in the long run, NO_x emissions should be
25 substantially reduced, approaching their maximum feasible reduction levels, in both the BTH
26 and its surrounding regions. Fourth, more stringent control policies should be enforced in
27 Southern Hebei, which on one hand suffers from the most severe $PM_{2.5}$ pollution (Wang et al.,
28 2014a), and on the other hand, significantly affects both local and regional $PM_{2.5}$
29 concentrations. Last but not least, considering the distinct source contributions in different
30 heavy pollution episodes, episode-specific temporary control strategies should be formulated
31 according to the source contribution feature of the specific pollution type.

32



1 Acknowledgements

2 This research has been supported by National Science Foundation of China (21625701 &
3 21521064), MOST National Key R & D program (2016YFC0207601), Strategic Pilot Project
4 of Chinese Academy of Sciences (XDB05030401), the UCLA Sustainable Los Angeles
5 Grand Challenge 2016 YZ-50958, and the Jet Propulsion Laboratory, California Institute of
6 Technology, under contract with NASA. The simulations were completed on the “Explorer
7 100” cluster system of Tsinghua National Laboratory for Information Science and
8 Technology.

10 References

- 11 Burnett, R. T., Pope, C. A., Ezzati, M., Olives, C., Lim, S. S., Mehta, S., Shin, H. H., Singh,
12 G., Hubbell, B., Brauer, M., Anderson, H. R., Smith, K. R., Balme, J. R., Bruce, N. G.,
13 Kan, H. D., Laden, F., Pruss-Ustun, A., Michelle, C. T., Gapstur, S. M., Diver, W. R.,
14 and Cohen, A.: An Integrated Risk Function for Estimating the Global Burden of
15 Disease Attributable to Ambient Fine Particulate Matter Exposure, *Environ Health*
16 *Persp*, 122, 397-403, Doi 10.1289/Ehp.1307049, 2014.
- 17 Cai, S. Y., Wang, Y. J., Zhao, B., Wang, S. X., Chang, X., and Hao, J. M.: The impact of the
18 "Air Pollution Prevention and Control Action Plan" on PM_{2.5} concentrations in Jing-
19 Jin-Ji region during 2012-2020, *Sci. Total. Environ.*, in press, DOI
20 10.1016/j.scitotenv.2016.11.188, 2016.
- 21 Cheng, I., Zhang, L., Blanchard, P., Dalziel, J., and Tordon, R.: Concentration-weighted
22 trajectory approach to identifying potential sources of speciated atmospheric mercury at
23 an urban coastal site in Nova Scotia, Canada, *Atmos Chem Phys*, 13, 6031-6048,
24 10.5194/acp-13-6031-2013, 2013.
- 25 Cheng, Y. F., Zheng, G. J., Wei, C., Mu, Q., Zheng, B., Wang, Z. B., Gao, M., Zhang, Q., He,
26 K. B., Carmichael, G., Pöschl, U., and Su, H.: Reactive nitrogen chemistry in aerosol
27 water as a source of sulfate during haze events in China, *Sci Adv*, 2, e1601530, DOI:
28 10.1126/sciadv.1601530, 2016.
- 29 Dong, X. Y., Li, J., Fu, J. S., Gao, Y., Huang, K., and Zhuang, G. S.: Inorganic aerosols
30 responses to emission changes in Yangtze River Delta, China, *Sci Total Environ*, 481,
31 522-532, DOI 10.1016/j.scitotenv.2014.02.076, 2014.
- 32 Fu, X., Wang, S. X., Zhao, B., Xing, J., Cheng, Z., Liu, H., and Hao, J. M.: Emission
33 inventory of primary pollutants and chemical speciation in 2010 for the Yangtze River
34 Delta region, China, *Atmos Environ*, 70, 39-50, DOI 10.1016/j.atmosenv.2012.12.034,
35 2013.
- 36 Guenther, A., Karl, T., Harley, P., Wiedinmyer, C., Palmer, P. I., and Geron, C.: Estimates of
37 global terrestrial isoprene emissions using MEGAN (Model of Emissions of Gases and
38 Aerosols from Nature), *Atmos Chem Phys*, 6, 3181-3210, 2006.
- 39 Hakami, A., Odman, M. T., and Russell, A. G.: High-order, direct sensitivity analysis of
40 multidimensional air quality models, *Environ Sci Technol*, 37, 2442-2452, DOI
41 10.1021/Es020677h, 2003.



- 1 Hakami, A., Seinfeld, J. H., Chai, T. F., Tang, Y. H., Carmichael, G. R., and Sandu, A.:
2 Adjoint sensitivity analysis of ozone nonattainment over the continental United States,
3 *Environ Sci Technol*, 40, 3855-3864, DOI 10.1021/Es052135g, 2006.
- 4 Han, X., Zhang, M. G., Zhu, L. Y., and Skorokhod, A.: Assessment of the impact of
5 emissions reductions on air quality over North China Plain, *Atmos Pollut Res*, 7, 249-
6 259, 10.1016/j.apr.2015.09.009, 2016.
- 7 Iman, R. L., Davenport, J. M., and Zeigler, D. K.: *Latin Hypercube Sampling (Program User's*
8 *Guide)*, Sandia National Laboratories, Albuquerque, NM, U.S., 78 pp., 1980.
- 9 Jia, Y. T., Rahn, K. A., He, K. B., Wen, T. X., and Wang, Y. S.: A novel technique for
10 quantifying the regional component of urban aerosol solely from its sawtooth cycles, *J*
11 *Geophys Res-Atmos*, 113, 10.1029/2008jd010389, 2008.
- 12 Li, J. W., and Han, Z. W.: A modeling study of severe winter haze events in Beijing and its
13 neighboring regions, *Atmos Res*, 170, 87-97, 10.1016/j.atmosres.2015.11.009, 2016.
- 14 Li, M., Zhang, Q., Kurokawa, J., Woo, J. H., He, K. B., Lu, Z., Ohara, T., Song, Y., Streets, D.
15 G., Carmichael, G. R., Cheng, Y. F., Hong, C. P., Huo, H., Jiang, X. J., Kang, S. C., Liu,
16 F., Su, H., and Zheng, B.: MIX: a mosaic Asian anthropogenic emission inventory for
17 the MICS-Asia and the HTAP projects, *Atmos Chem Phys Discuss*, 15, 34813-34869,
18 doi:10.5194/acpd-15-34813-2015, 2015a.
- 19 Li, X., Zhang, Q., Zhang, Y., Zheng, B., Wang, K., Chen, Y., Wallington, T. J., Han, W. J.,
20 Shen, W., Zhang, X. Y., and He, K. B.: Source contributions of urban PM_{2.5} in the
21 Beijing-Tianjin-Hebei region: Changes between 2006 and 2013 and relative impacts of
22 emissions and meteorology, *Atmos Environ*, 123, 229-239,
23 10.1016/j.atmosenv.2015.10.048, 2015b.
- 24 Lim, S. S., Vos, T., Flaxman, A. D., Danaei, G., Shibuya, K., Adair-Rohani, H., AlMazroa, M.
25 A., Amann, M., Anderson, H. R., Andrews, K. G., Aryee, M., Atkinson, C., Bacchus, L.
26 J., Bahalim, A. N., Balakrishnan, K., Balmes, J., Barker-Collo, S., Baxter, A., Bell, M.
27 L., Blore, J. D., Blyth, F., Bonner, C., Borges, G., Bourne, R., Boussinesq, M., Brauer,
28 M., Brooks, P., Bruce, N. G., Brunekreef, B., Bryan-Hancock, C., Bucello, C.,
29 Buchbinder, R., Bull, F., Burnett, R. T., Byers, T. E., Calabria, B., Carapetis, J.,
30 Carnahan, E., Chafe, Z., Charlson, F., Chen, H., Chen, J. S., Cheng, A. T.-A., Child, J.
31 C., Cohen, A., Colson, K. E., Cowie, B. C., Darby, S., Darling, S., Davis, A.,
32 Degenhardt, L., Dentener, F., Des Jarlais, D. C., Devries, K., Dherani, M., Ding, E. L.,
33 Dorsey, E. R., Driscoll, T., Edmond, K., Ali, S. E., Engell, R. E., Erwin, P. J., Fahimi, S.,
34 Falder, G., Farzadfar, F., Ferrari, A., Finucane, M. M., Flaxman, S., Fowkes, F. G. R.,
35 Freedman, G., Freeman, M. K., Gakidou, E., Ghosh, S., Giovannucci, E., Gmel, G.,
36 Graham, K., Grainger, R., Grant, B., Gunnell, D., Gutierrez, H. R., Hall, W., Hoek, H.
37 W., Hogan, A., Hosgood Iii, H. D., Hoy, D., Hu, H., Hubbell, B. J., Hutchings, S. J.,
38 Ibeanusi, S. E., Jacklyn, G. L., Jasrasaria, R., Jonas, J. B., Kan, H., Kanis, J. A.,
39 Kassebaum, N., Kawakami, N., Khang, Y.-H., Khatibzadeh, S., Khoo, J.-P., Kok, C.,
40 Laden, F., Lalloo, R., Lan, Q., Lathlean, T., Leasher, J. L., Leigh, J., Li, Y., Lin, J. K.,
41 Lipshultz, S. E., London, S., Lozano, R., Lu, Y., Mak, J., Malekzadeh, R., Mallinger, L.,
42 Marcenés, W., March, L., Marks, R., Martin, R., McGale, P., McGrath, J., Mehta, S.,
43 Memish, Z. A., Mensah, G. A., Merriman, T. R., Micha, R., Michaud, C., Mishra, V.,
44 Hanafiah, K. M., Mokdad, A. A., Morawska, L., Mozaffarian, D., Murphy, T., Naghavi,
45 M., Neal, B., Nelson, P. K., Nolla, J. M., Norman, R., Olives, C., Omer, S. B., Orchard,
46 J., Osborne, R., Ostro, B., Page, A., Pandey, K. D., Parry, C. D. H., Passmore, E., Patra,
47 J., Pearce, N., Pelizzari, P. M., Petzold, M., Phillips, M. R., Pope, D., Pope Iii, C. A.,
48 Powles, J., Rao, M., Razavi, H., Rehfuess, E. A., Rehm, J. T., Ritz, B., Rivara, F. P.,



- 1 Roberts, T., Robinson, C., Rodriguez-Portales, J. A., Romieu, I., Room, R., Rosenfeld,
2 L. C., Roy, A., Rushton, L., Salomon, J. A., Sampson, U., Sanchez-Riera, L., Sanman,
3 E., Sapkota, A., Seedat, S., Shi, P., Shield, K., Shivakoti, R., Singh, G. M., Sleet, D. A.,
4 Smith, E., Smith, K. R., Stapelberg, N. J. C., Steenland, K., Stöckl, H., Stovner, L. J.,
5 Straif, K., Straney, L., Thurston, G. D., Tran, J. H., Van Dingenen, R., van Donkelaar,
6 A., Veerman, J. L., Vijayakumar, L., Weintraub, R., Weissman, M. M., White, R. A.,
7 Whiteford, H., Wiersma, S. T., Wilkinson, J. D., Williams, H. C., Williams, W., Wilson,
8 N., Woolf, A. D., Yip, P., Zielinski, J. M., Lopez, A. D., Murray, C. J. L., and Ezzati,
9 M.: A comparative risk assessment of burden of disease and injury attributable to 67 risk
10 factors and risk factor clusters in 21 regions, 1990–2010: a systematic analysis for the
11 Global Burden of Disease Study 2010, *The Lancet*, 380, 2224-2260,
12 [http://dx.doi.org/10.1016/S0140-6736\(12\)61766-8](http://dx.doi.org/10.1016/S0140-6736(12)61766-8), 2012.
- 13 Liu, J., Mauzerall, D. L., Chen, Q., Zhang, Q., Song, Y., Peng, W., Klimont, Z., Qiu, X. H.,
14 Zhang, S. Q., Hu, M., Lin, W. L., Smith, K. R., and Zhu, T.: Air pollutant emissions
15 from Chinese households: A major and underappreciated ambient pollution source, *P*
16 *Natl Acad Sci USA*, 113, 7756-7761, 10.1073/pnas.1604537113, 2016.
- 17 Lv, L. Y., and Li, H. Y.: Economic evaluation of the health effect of PM10 and PM2.5
18 pollution over the Beijing-Tianjin-Hebei region, *Acta Scientiarum Naturalium*
19 *Universitatis Nankaiensis*, 69-77, 2016.
- 20 Russell, A., Milford, J., Bergin, M. S., McBride, S., Mcnair, L., Yang, Y., Stockwell, W. R.,
21 and Croes, B.: Urban Ozone Control and Atmospheric Reactivity of Organic Gases,
22 *Science*, 269, 491-495, DOI 10.1126/science.269.5223.491, 1995.
- 23 Sandu, A., Daescu, D. N., Carmichael, G. R., and Chai, T. F.: Adjoint sensitivity analysis of
24 regional air quality models, *J Comput Phys*, 204, 222-252, DOI
25 10.1016/j.jcp.2004.10.011, 2005.
- 26 Santner, T. J., Williams, B. J., and Notz, W.: *The Design and Analysis of Computer*
27 *Experiments*, Springer Verlag, New York, U.S., 283 pp., 2003.
- 28 Stein, A. F., Draxler, R. R., Rolph, G. D., Stunder, B. J. B., Cohen, M. D., and Ngan, F.:
29 NOAA's HYSPLIT atmospheric transport and dispersion modeling system, *B Am*
30 *Meteorol Soc*, 96, 2059-2077, 10.1175/bams-d-14-00110.1, 2015.
- 31 Stocker, T. F., Qin, D., Plattner, G.-K., Tignor, M., Allen, S. K., Boschung, J., Nauels, A., Xia,
32 Y., Bex, V., and Midgley, P. M.: *Climate Change 2013: The Physical Science Basis.*
33 *Contribution of Working Group I to the Fifth Assessment Report of the*
34 *Intergovernmental Panel on Climate Change*, Cambridge University Press, Cambridge,
35 United Kingdom and New York, NY, USA, 1535 pp., 2013.
- 36 Streets, D. G., Fu, J. S., Jang, C. J., Hao, J. M., He, K. B., Tang, X. Y., Zhang, Y. H., Wang,
37 Z. F., Li, Z. P., and Zhang, Q.: Air quality during the 2008 Beijing Olympic Games,
38 *Atmos Environ*, 41, 480-492, DOI 10.1016/j.atmosenv.2006.08.046, 2007.
- 39 The State Council of the People's Republic of China: Notice to issue the "Air Pollution
40 Prevention and Control Action Plan": [http://www.gov.cn/zwqk/2013-](http://www.gov.cn/zwqk/2013-09/12/content_2486773.htm)
41 [09/12/content_2486773.htm](http://www.gov.cn/zwqk/2013-09/12/content_2486773.htm), access: September 9, 2016, 2013.
- 42 U.S. Environmental Protection Agency: Technical support document for the proposed PM
43 NAAQS rule: Response Surface Modeling[R/OL]:
44 http://www.epa.gov/scram001/reports/pmnaaqs_tsd_rsm_all_021606.pdf, access: 2015-
45 02-01, 2006.
- 46 van Donkelaar, A., Martin, R. V., Brauer, M., and Boys, B. L.: Use of satellite observations
47 for long-term exposure assessment of global concentrations of fine particulate matter,
48 *Environmental health perspectives*, 123, 135, 2015.



- 1 Wang, G. H., Zhang, R. Y., Gomez, M. E., Yang, L. X., Zamora, M. L., Hu, M., Lin, Y., Peng,
2 J. F., Guo, S., Meng, J. J., Li, J. J., Cheng, C. L., Hu, T. F., Ren, Y. Q., Wang, Y. S.,
3 Gao, J., Cao, J. J., An, Z. S., Zhou, W. J., Li, G. H., Wang, J. Y., Tian, P. F., Marrero-
4 Ortiz, W., Secretst, J., Du, Z. F., Zheng, J., Shang, D. J., Zeng, L. M., Shao, M., Wang,
5 W. G., Huang, Y., Wang, Y., Zhu, Y. J., Li, Y. X., Hu, J. X., Pan, B., Cai, L., Cheng, Y.
6 T., Ji, Y. M., Zhang, F., Rosenfeld, D., Liss, P. S., Duce, R. A., Kolb, C. E., and Molina,
7 M. J.: Persistent sulfate formation from London Fog to Chinese haze, *P Natl Acad Sci*
8 *USA*, 113, 13630-13635, 10.1073/pnas.1616540113, 2016a.
- 9 Wang, J. D., Xing, J., Mathur, R., Pleim, J. E., Wang, S. X., Hogrefe, C., Gan, C.-M., Wong,
10 D. C., and Hao, J. M.: Historical Trends in PM_{2.5}-Related Premature Mortality during
11 1990-2010 across the Northern Hemisphere, *Environ Health Persp*, in press, DOI
12 10.1289/EHP298, 2016b.
- 13 Wang, J. D., Zhao, B., Yang, F. M., Xing, J., Morawska, L., Ding, A. J., Kulmala, M.,
14 Kerminen, V.-M., Kujansuu, J., Wang, Z. F., Ding, D., Zhang, X. Y., Wang, H. B., Tian,
15 M., Petäjä, T., Jiang, J. K., and Hao, J. M.: Particulate matter pollution over China and
16 the effects of control policies, *Sci Total Environ*, in press, DOI
17 10.1016/j.scitotenv.2017.01.027, 2017.
- 18 Wang, L. T., Hao, J. M., He, K. B., Wang, S. X., Li, J. H., Zhang, Q., Streets, D. G., Fu, J. S.,
19 Jang, C. J., Takekawa, H., and Chatani, S.: A modeling study of coarse particulate
20 matter pollution in Beijing: Regional source contributions and control implications for
21 the 2008 summer Olympics, *J Air Waste Manage*, 58, 1057-1069, Doi 10.3155/1047-
22 3289.58.8.1057, 2008.
- 23 Wang, L. T., Wei, Z., Yang, J., Zhang, Y., Zhang, F. F., Su, J., Meng, C. C., and Zhang, Q.:
24 The 2013 severe haze over southern Hebei, China: model evaluation, source
25 apportionment, and policy implications, *Atmos Chem Phys*, 14, 3151-3173,
26 10.5194/acp-14-3151-2014, 2014a.
- 27 Wang, S. X., Xing, J., Jang, C. R., Zhu, Y., Fu, J. S., and Hao, J. M.: Impact assessment of
28 ammonia emissions on inorganic aerosols in east China using response surface modeling
29 technique, *Environ Sci Technol*, 45, 9293-9300, DOI 10.1021/Es2022347, 2011.
- 30 Wang, S. X., Zhao, B., Cai, S. Y., Klimont, Z., Nielsen, C. P., Morikawa, T., Woo, J. H., Kim,
31 Y., Fu, X., Xu, J. Y., Hao, J. M., and He, K. B.: Emission trends and mitigation options
32 for air pollutants in East Asia, *Atmos Chem Phys*, 14, 6571-6603, DOI 10.5194/acp-14-
33 6571-2014, 2014b.
- 34 Wang, Y. J., Bao, S. W., Wang, S. X., Hu, Y. T., Shi, X., Wang, J. D., Zhao, B., Jiang, J. K.,
35 Zheng, M., Wu, M. H., Russell, A. G., Wang, Y. H., and Hao, J. M.: Local and regional
36 contributions to fine particulate matter in Beijing during heavy haze episodes, *Sci Total*
37 *Environ*, in press, DOI: 10.1016/j.scitotenv.2016.12.127, 2016c.
- 38 Wu, W. J.: Health Effect Attributed to Ambient Fine Particle Pollution in the Beijing-Tianjin-
39 Hebei Region and its Source Apportionment, Doctor, School of Environment, Tsinghua
40 University, Beijing, China, 98 pp., 2016.
- 41 Xing, J., Wang, S. X., Jang, C., Zhu, Y., and Hao, J. M.: Nonlinear response of ozone to
42 precursor emission changes in China: a modeling study using response surface
43 methodology, *Atmos Chem Phys*, 11, 5027-5044, DOI 10.5194/acp-11-5027-2011,
44 2011.
- 45 Yang, Y. J., Wilkinson, J. G., and Russell, A. G.: Fast, direct sensitivity analysis of
46 multidimensional photochemical models, *Environ Sci Technol*, 31, 2859-2868, DOI
47 10.1021/Es970117w, 1997.



- 1 Ying, Q., Wu, L., and Zhang, H. L.: Local and inter-regional contributions to PM_{2.5} nitrate
2 and sulfate in China, *Atmos Environ*, 94, 582-592, 10.1016/j.atmosenv.2014.05.078,
3 2014.
- 4 Yu, L. D., Wang, G. F., Zhang, R. J., Zhang, L. M., Song, Y., Wu, B. B., Li, X. F., An, K.,
5 and Chu, J. H.: Characterization and Source Apportionment of PM_{2.5} in an Urban
6 Environment in Beijing, *Aerosol Air Qual Res*, 13, 574-583, 10.4209/aaqr.2012.07.0192,
7 2013.
- 8 Zhang, L., Shao, J. Y., Lu, X., Zhao, Y. H., Hu, Y. Y., Henze, D. K., Liao, H., Gong, S. L.,
9 and Zhang, Q.: Sources and Processes Affecting Fine Particulate Matter Pollution over
10 North China: An Adjoint Analysis of the Beijing APEC Period, *Environ Sci Technol*, 50,
11 8731-8740, 10.1021/acs.est.6b03010, 2016.
- 12 Zhang, W., Guo, J. H., Sun, Y. L., Yuan, H., Zhuang, G. S., Zhuang, Y. H., and Hao, Z. P.:
13 Source apportionment for urban PM₁₀ and PM_{2.5} in the Beijing area, *Chinese Sci Bull*,
14 52, 608-615, 10.1007/s11434-007-0076-5, 2007.
- 15 Zhao, B., Wang, S. X., Dong, X. Y., Wang, J. D., Duan, L., Fu, X., Hao, J. M., and Fu, J.:
16 Environmental effects of the recent emission changes in China: implications for
17 particulate matter pollution and soil acidification, *Environ Res Lett*, 8, 024031, DOI
18 10.1088/1748-9326/8/2/024031, 2013a.
- 19 Zhao, B., Wang, S. X., Liu, H., Xu, J. Y., Fu, K., Klimont, Z., Hao, J. M., He, K. B., Cofala,
20 J., and Amann, M.: NO_x emissions in China: historical trends and future perspectives,
21 *Atmos Chem Phys*, 13, 9869-9897, DOI 10.5194/acp-13-9869-2013, 2013b.
- 22 Zhao, B., Wang, S. X., Wang, J. D., Fu, J. S., Liu, T. H., Xu, J. Y., Fu, X., and Hao, J. M.:
23 Impact of national NO_x and SO₂ control policies on particulate matter pollution in
24 China, *Atmos Environ*, 77, 453-463, DOI 10.1016/j.atmosenv.2013.05.012, 2013c.
- 25 Zhao, B., Wang, S. X., Donahue, N. M., Chuang, W., Hildebrandt Ruiz, L., Ng, N. L., Wang,
26 Y. J., and Hao, J. M.: Evaluation of one-dimensional and two-dimensional volatility
27 basis sets in simulating the aging of secondary organic aerosols with smog-chamber
28 experiments, *Environ Sci Technol*, 49, 2245-2254, DOI 10.1021/es5048914, 2015a.
- 29 Zhao, B., Wang, S. X., Xing, J., Fu, K., Fu, J. S., Jang, C., Zhu, Y., Dong, X. Y., Gao, Y., Wu,
30 W. J., Wang, J. D., and Hao, J. M.: Assessing the nonlinear response of fine particles to
31 precursor emissions: development and application of an extended response surface
32 modeling technique v1.0, *Geosci Model Dev*, 8, 115-128, DOI 10.5194/gmd-8-115-
33 2015, 2015b.
- 34 Zhao, B., Wang, S. X., Donahue, N. M., Jathar, S. H., Huang, X. F., Wu, W. J., Hao, J. M.,
35 and Robinson, A. L.: Quantifying the effect of organic aerosol aging and intermediate-
36 volatility emissions on regional-scale aerosol pollution in China, *Sci Rep-Uk*, 6,
37 10.1038/srep28815, 2016.
- 38 Zhao, Y., Wang, S. X., Duan, L., Lei, Y., Cao, P. F., and Hao, J. M.: Primary air pollutant
39 emissions of coal-fired power plants in China: Current status and future prediction,
40 *Atmos Environ*, 42, 8442-8452, DOI 10.1016/j.atmosenv.2008.08.021, 2008.
- 41 Zheng, G. J., Duan, F. K., Su, H., Ma, Y. L., Cheng, Y., Zheng, B., Zhang, Q., Huang, T.,
42 Kimoto, T., Chang, D., Poschl, U., Cheng, Y. F., and He, K. B.: Exploring the severe
43 winter haze in Beijing: the impact of synoptic weather, regional transport and
44 heterogeneous reactions, *Atmos Chem Phys*, 15, 2969-2983, 10.5194/acp-15-2969-2015,
45 2015.
- 46
47
48



1 **Tables and figures**

2 Table 1. Description of the RSM/ERSM prediction systems developed in this study.

Method	Control variables	Control scenarios
Conventional RSM technique	5 control variables: total emissions of NO _x , SO ₂ , NH ₃ , NMVOC+IVOC, and POA	101 control scenarios: 1) 1 CMAQ/2D-VBS base case; 2) 100 ^a scenarios generated by applying LHS method for the 5 variables.
ERSM technique	55 control variables in total: 11 control variables in each of the 5 regions, including 7 nonlinear control variables, i.e., 1) NO _x /large point sources (LPS) ^b 2) NO _x /other sources 3) SO ₂ /LPS 4) SO ₂ /other sources 5) NH ₃ /all sources 6) NMVOC+IVOC/all sources 7) POA/all sources and 4 linear control variables, i.e., 8) Primary inorganic PM _{2.5} /power plants 9) Primary inorganic PM _{2.5} /Industry 10) Primary inorganic PM _{2.5} /residential & commercial 11) Primary inorganic PM _{2.5} /transportation	1121 control scenarios: 1) 1 CMAQ/2D-VBS base case; 2) 1000 scenarios, including 200 ^a scenarios generated by applying LHS method for the nonlinear control variables in Beijing, 200 scenarios generated in the same way for Tianjin, 200 scenarios for Northern Hebei, 200 scenarios for Southern Hebei, and 200 scenarios for Eastern Hebei; 3) 100 ^a scenarios generated by applying LHS method for the total emissions of NO _x , SO ₂ , NH ₃ , NMVOC+IVOC, and POA; 4) 20 scenarios where one primary inorganic PM _{2.5} control variable is set to 0.25 for each scenario.

3 ^a 100 and 200 scenarios are needed for the response surfaces for 5 and 7 variables, respectively (Xing et al.,
 4 2011; Wang et al., 2011).

5 ^b LPS includes power plants, iron and steel plants, and cement plants

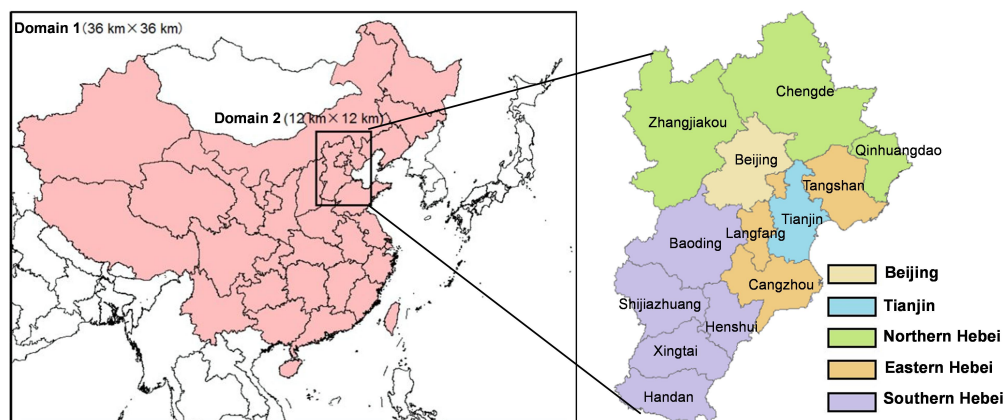
6



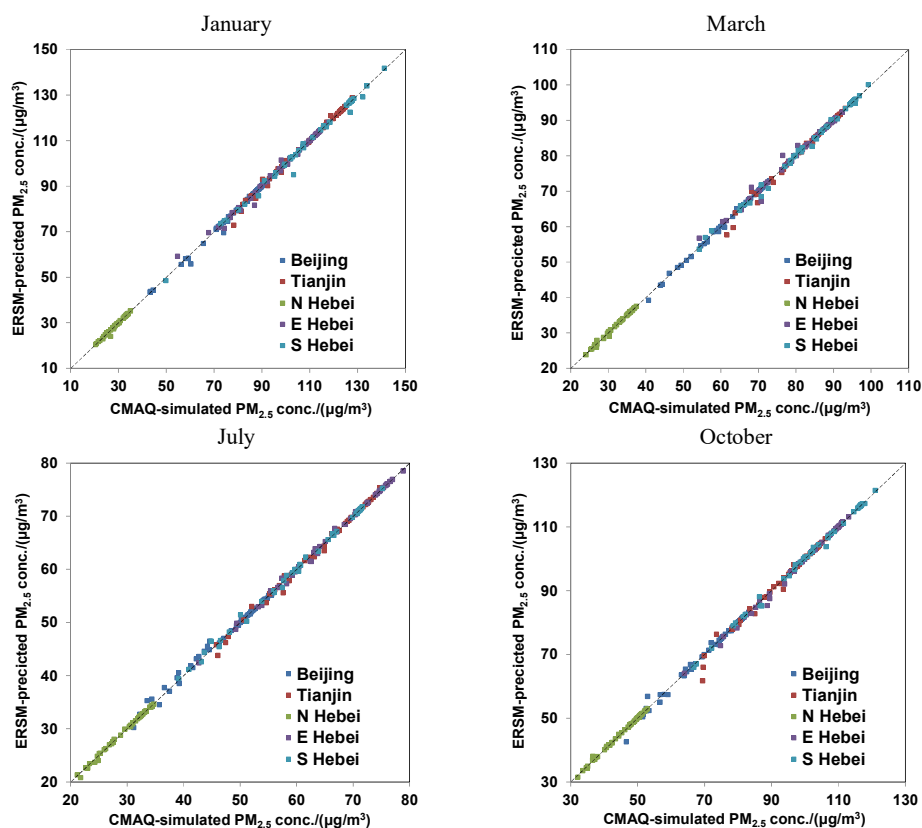
1 Table 2. Comparison between ERSM-predicted and CMAQ/2D-VBS-simulated PM_{2.5} concentrations for
2 54 out-of-sample scenarios.

Month	Variable	Statistical index	Beijing	Tianjin	Northern Hebei	Eastern Hebei	Southern Hebei
Jan	PM _{2.5} concentration	R	0.998	0.998	0.995	0.997	0.997
		MNE (%)	0.52	0.55	0.64	0.67	0.60
		Maximum NE (%)	7.56	6.98	10.67	8.01	8.03
		95% percentile of NEs (%)	1.61	2.86	2.92	3.46	3.02
		NME (%)	0.44	0.46	0.57	0.53	0.53
PM _{2.5} response	NME (%)	3.36	3.48	4.25	4.00	3.88	
Mar	PM _{2.5} concentration	R	0.999	0.996	0.998	0.995	0.999
		MNE (%)	0.37	0.54	0.39	0.57	0.49
		Maximum NE (%)	3.75	6.58	4.30	5.04	3.22
		95% percentile of NEs (%)	1.53	3.15	2.03	4.35	2.03
		NME (%)	0.31	0.45	0.34	0.49	0.42
PM _{2.5} response	NME (%)	2.38	4.32	2.70	4.55	3.59	
Jul	PM _{2.5} concentration	R	0.997	0.998	0.998	0.999	0.999
		MNE (%)	0.94	0.54	0.46	0.37	0.47
		Maximum NE (%)	5.05	5.02	4.65	1.83	3.62
		95% percentile of NEs (%)	3.47	2.33	2.17	1.49	1.87
		NME (%)	0.80	0.47	0.41	0.33	0.39
PM _{2.5} response	NME (%)	4.97	3.71	2.80	2.58	2.78	
Oct	PM _{2.5} concentration	R	0.996	0.994	0.999	0.999	0.999
		MNE (%)	0.83	0.70	0.36	0.39	0.36
		Maximum NE (%)	8.90	11.19	3.79	3.90	2.46
		95% percentile of NEs (%)	3.04	3.50	1.44	2.10	1.64
		NME (%)	0.67	0.58	0.30	0.35	0.32
PM _{2.5} response	NME (%)	4.51	5.64	2.20	3.29	2.79	

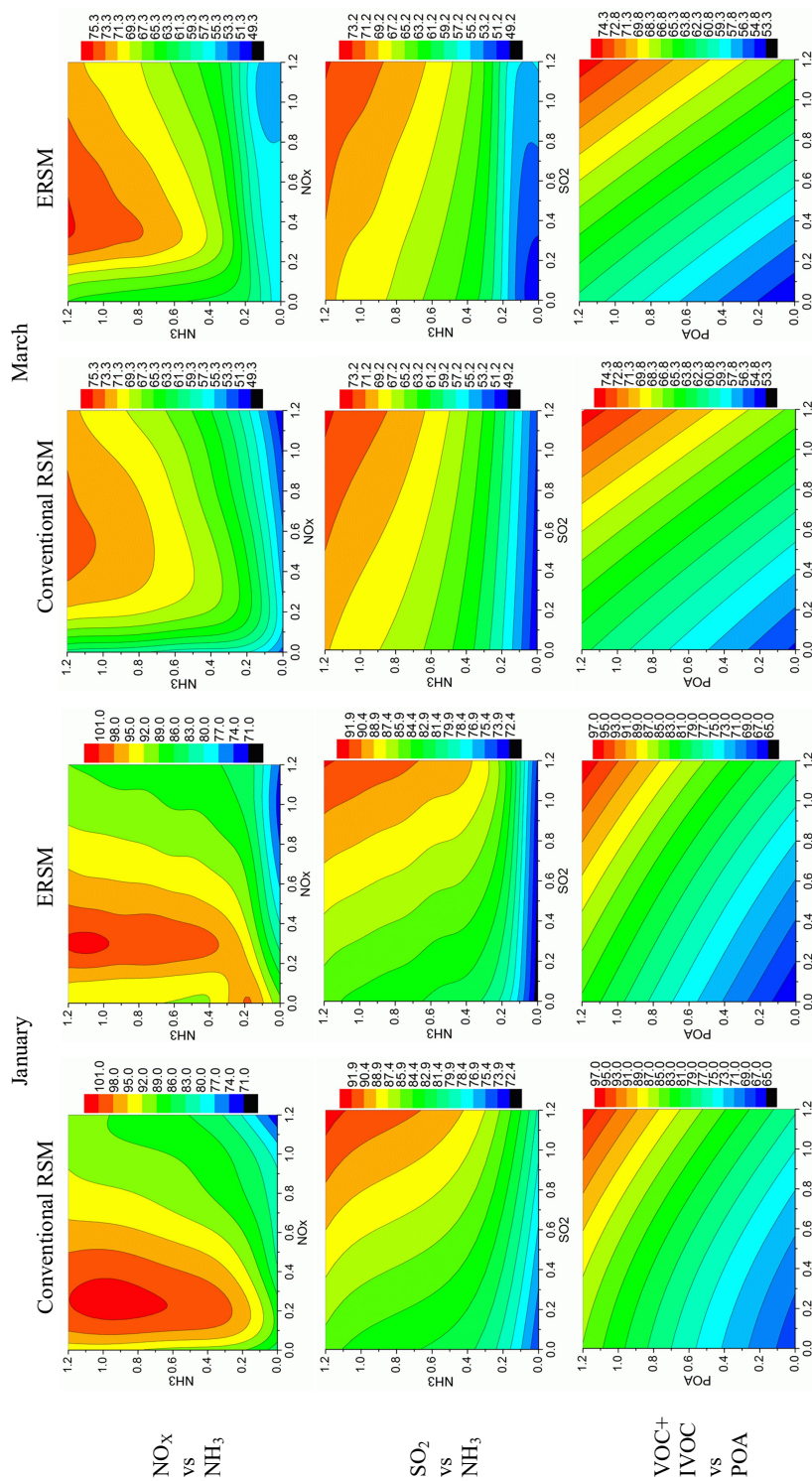
3



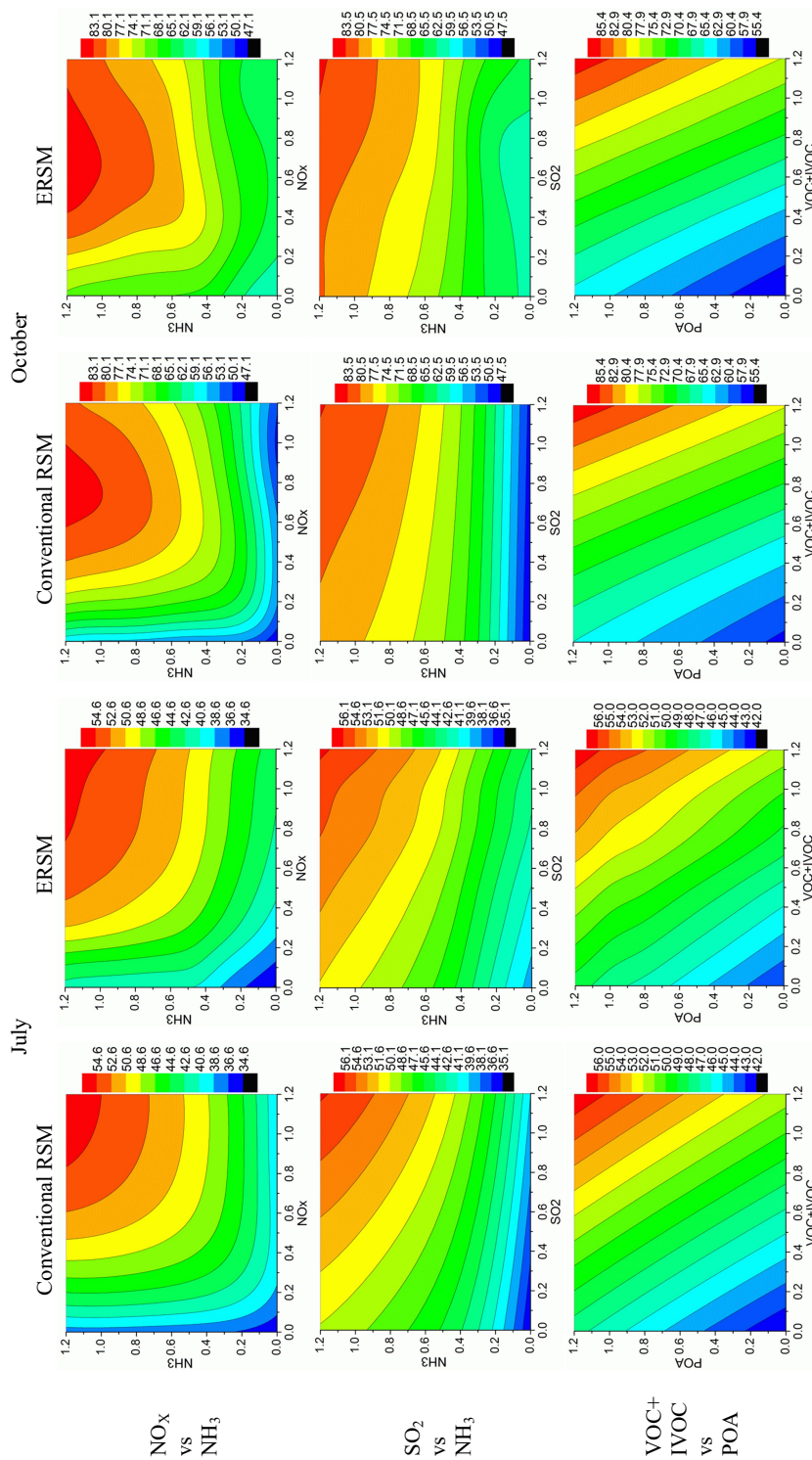
1
2 Figure 1. Double nesting domains used in CMAQ/2D-VBS simulation (left) and the definition
3 of five target regions in the innermost domain, denoted by different colours (right). The grey
4 lines in the right figure represent the boundaries of prefecture-level cities.
5



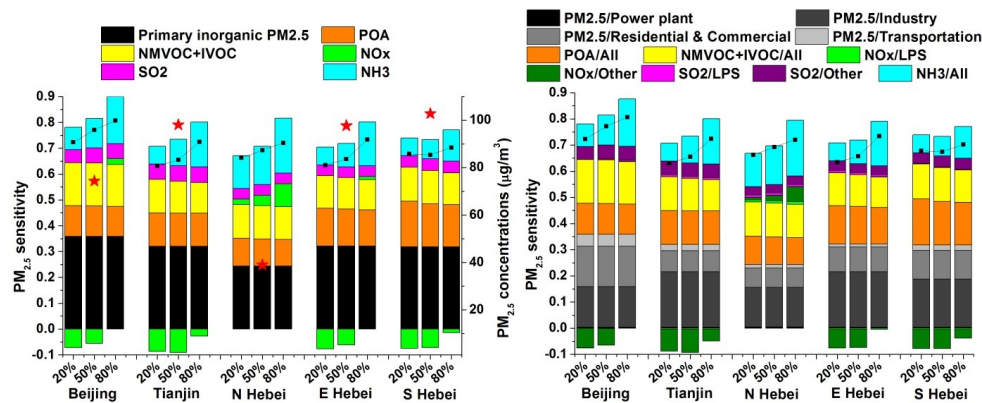
1 Figure 2. Comparison of $PM_{2.5}$ concentrations predicted by the ERSM technique with out-of-
2 sample CMAQ/2D-VBS simulations. The dashed line is the one-to-one line indicating perfect
3 agreement.



1 Figure 3. Comparison of the 2-D isopleths of $PM_{2.5}$ concentrations in Beijing in response to the simultaneous changes of precursor
 2 emissions in all five regions derived from the conventional RSM technique and the ERSM technique. The X- and Y-axis represent the
 3 emission ratio, defined as the ratios of the changed emissions to the emissions in the base case. The colour contours represent $PM_{2.5}$
 4 concentrations (unit: $\mu g m^{-3}$).

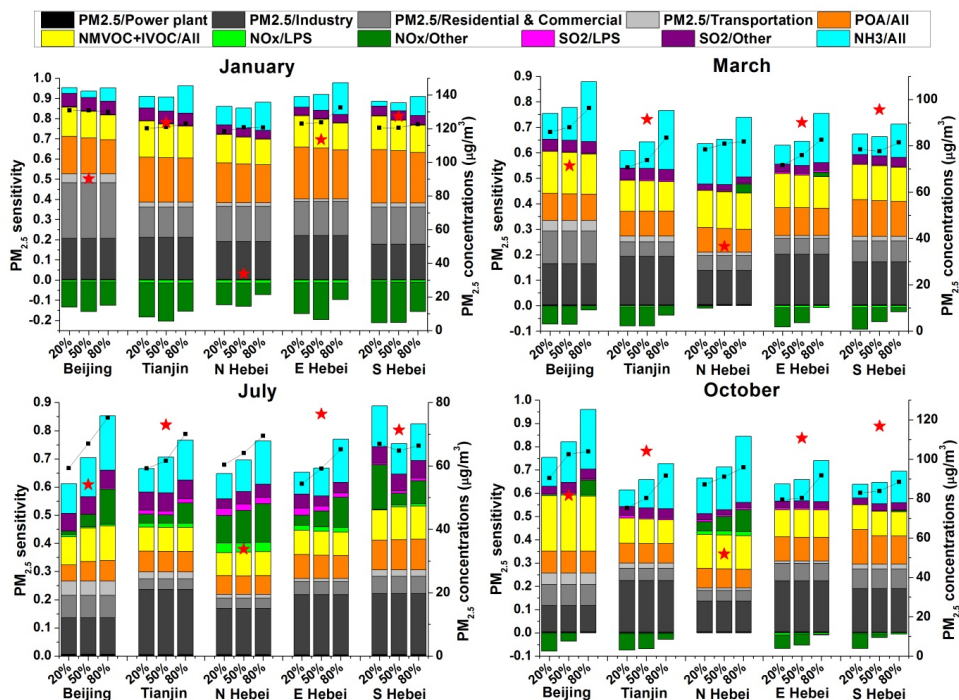


2 Figure 3. Continued.



1
 2 Figure 4. Sensitivity of 4-month mean $PM_{2.5}$ concentrations to stepped control of individual
 3 air pollutants (left) and individual pollutant-sector combinations (right). The X-axis shows the
 4 reduction ratio ($= 1 - \text{emission ratio}$). The Y-axis shows $PM_{2.5}$ sensitivity, which is defined as
 5 the change ratio of concentration divided by the reduction ratio of emissions. The coloured
 6 bars denote the $PM_{2.5}$ sensitivities when a particular emission source is controlled while the
 7 others stay the same as the base case; the black dotted line denotes the $PM_{2.5}$ sensitivity when
 8 all emission sources are controlled simultaneously. The red stars represent $PM_{2.5}$
 9 concentrations in the base case.

10



1
 2 Figure 5. Sensitivity of monthly mean $PM_{2.5}$ concentrations to stepped control of individual
 3 air pollutants from individual sectors in January, March, July, and October. The meanings of
 4 X-axis, Y-axis, coloured bars, black dotted lines, and red stars are the same as Fig. 4.
 5

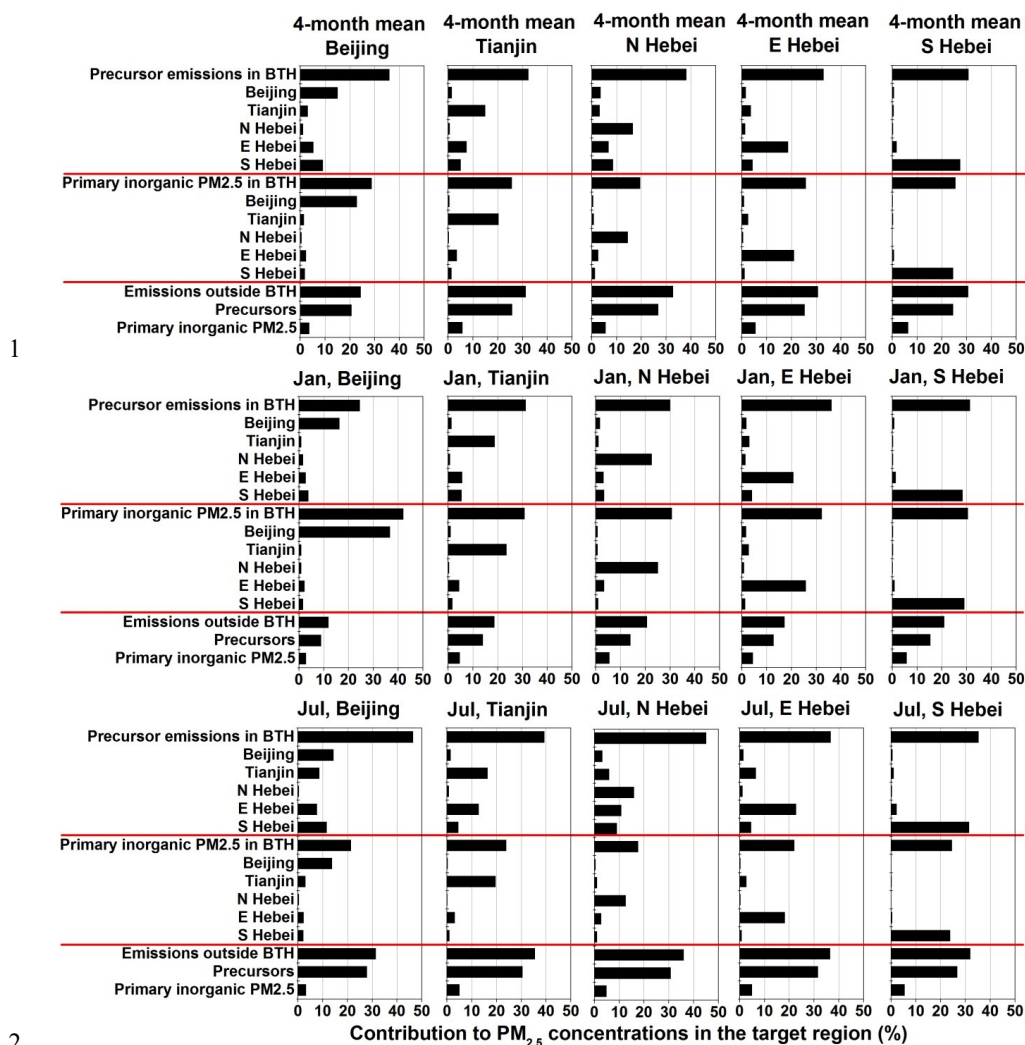
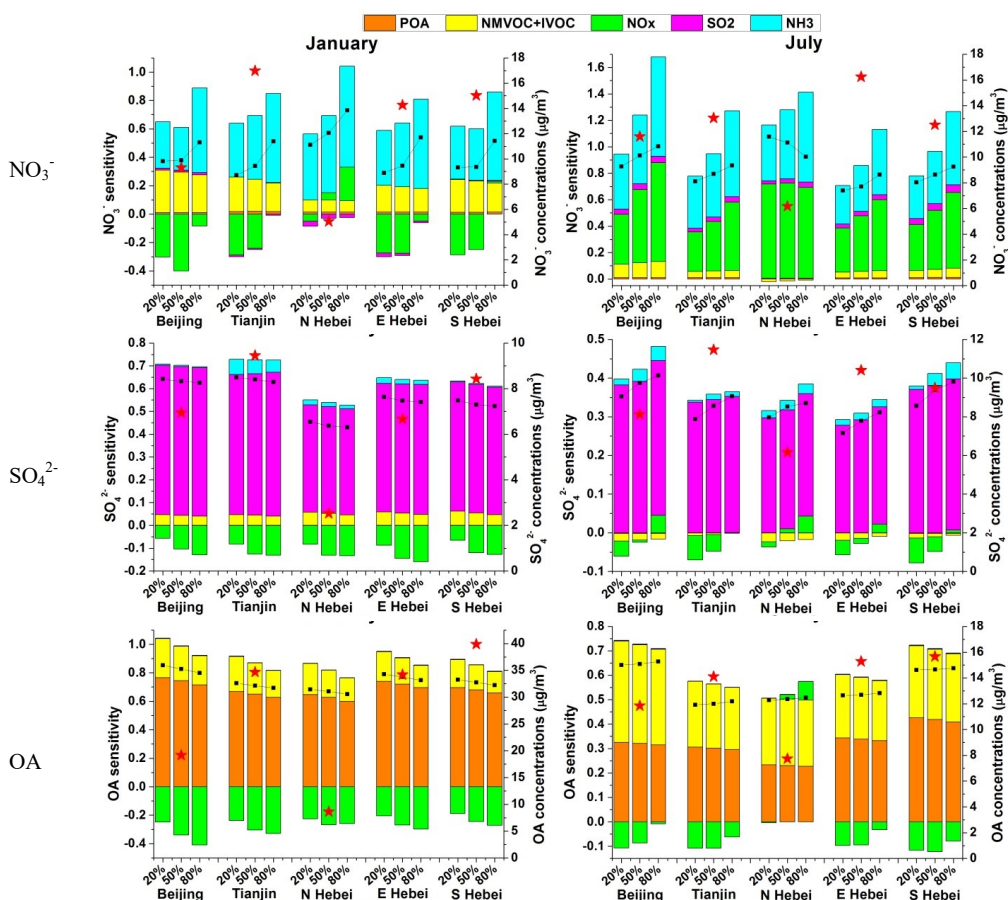


Figure 6. Contributions of precursor (NO_x , SO_2 , NH_3 , NMVOC, IVOC, and POA) and primary inorganic $\text{PM}_{2.5}$ emissions from individual regions to $\text{PM}_{2.5}$ concentrations. The contributions are quantified by comparing the base case with sensitivity scenarios in which emissions from a specific source are reduced by 80%. This figure illustrates contributions to 4-month mean $\text{PM}_{2.5}$ concentrations and monthly mean $\text{PM}_{2.5}$ concentrations in January and July. The results for March and October are given in Fig. S6.



1 Figure 7. Sensitivity of monthly mean NO_3^- , SO_4^{2-} , and OA concentrations to stepped control
 2 of individual air pollutants in January and July. The meanings of X-axis, Y-axis, coloured
 3 bars, black dotted lines, and red stars are the same as Fig. 4 but for $\text{NO}_3^-/\text{SO}_4^{2-}/\text{OA}$. The
 4 results for March and October are given in Fig. S7.
 5

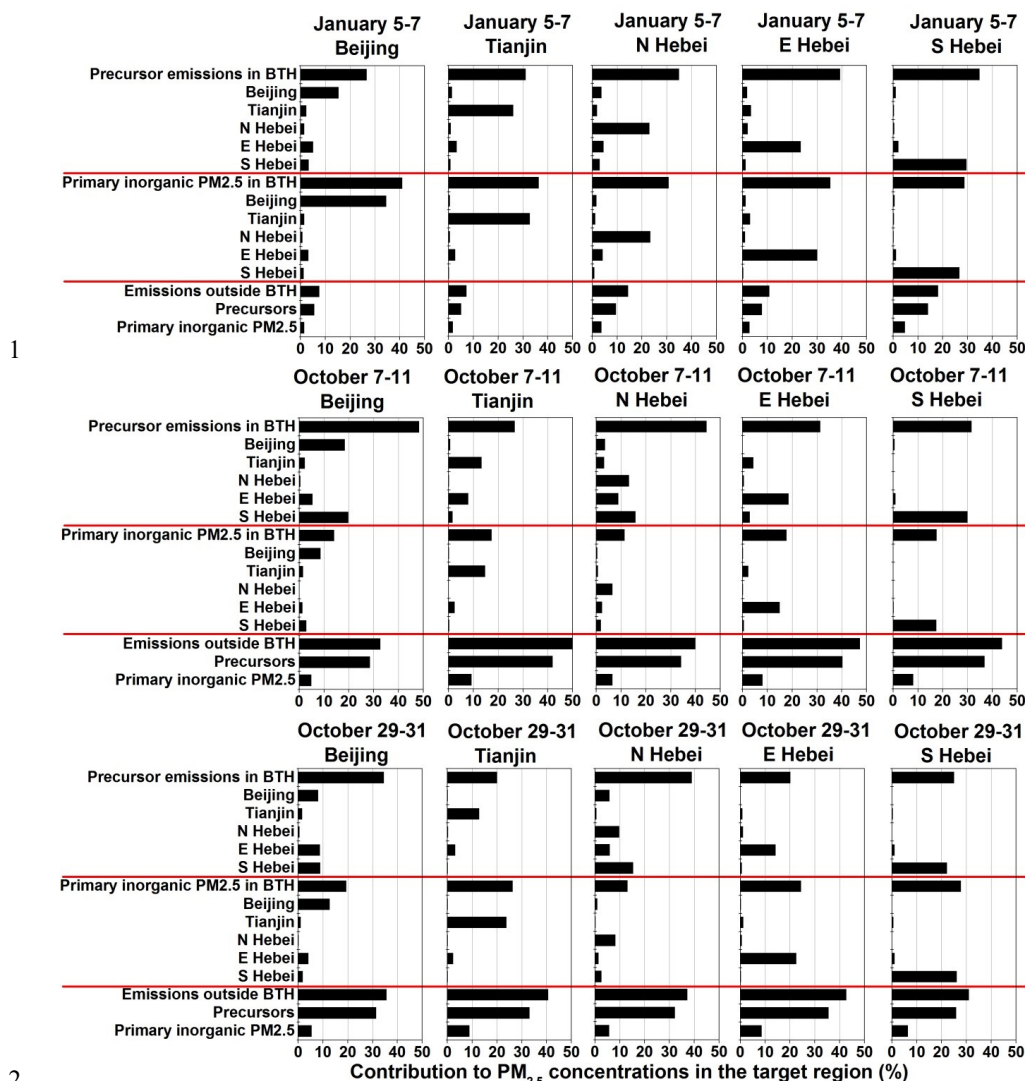
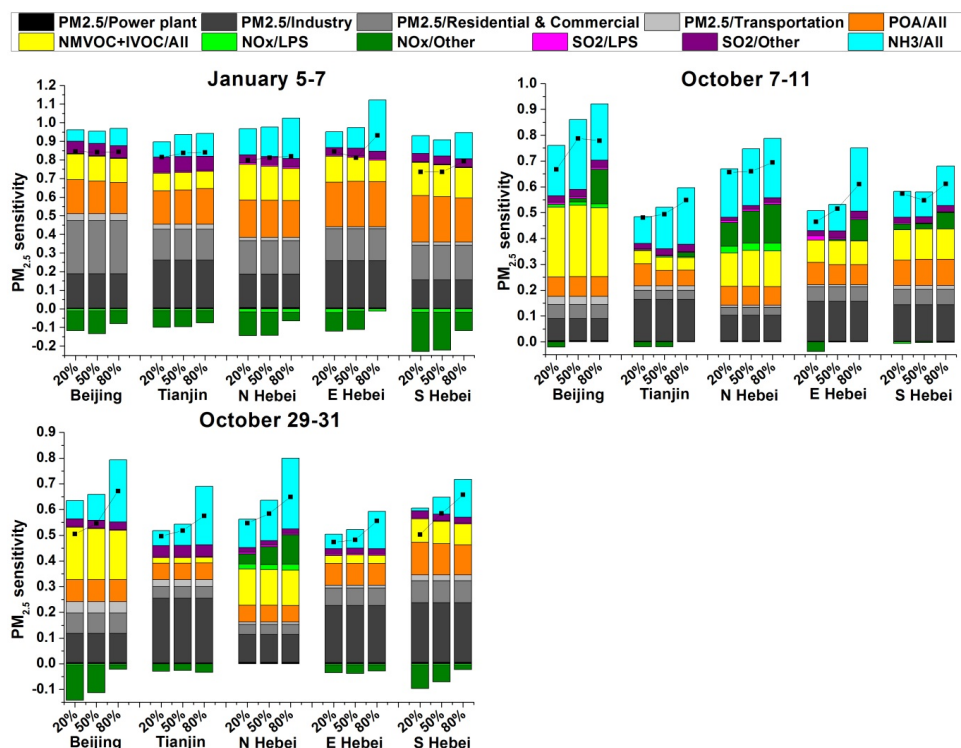


Figure 8. Contribution of precursor (NO_x , SO_2 , NH_3 , NMVOC, IVOC, and POA) and primary inorganic $\text{PM}_{2.5}$ emissions from individual regions to $\text{PM}_{2.5}$ concentrations during three typical heavy-pollution episodes.



1
 2 Figure 9. Sensitivity of $PM_{2.5}$ concentrations to stepped control of individual air pollutants
 3 from individual sectors during three heavy-pollution episodes. The meanings of X-axis, Y-
 4 axis, coloured bars, and black dotted lines are the same as Fig. 4.
 5